

NON-DIFFRACTING WAVES: A NEW INTRODUCTION^(†)

Erasmus Recami^{1,2,3}, M.Zamboni-Rached^{4,1}, H.E.Hernández-Figueroa¹, and L.A.Ambrósio⁵

¹ *DECOM, FEEC, Universidade Estadual de Campinas (UNICAMP), Campinas, SP, Brazil*

² *Facoltà di Ingegneria, Università statale di Bergamo, Bergamo, Italy.*

³ *INFN—Sezione di Milano, Milan, Italy.*

⁴ *Photonics Group, Electrical & Computer Engineering, University of Toronto, Canada.*

⁵ *SEL, EESC, University of Sao Paulo (USP), Sao Carlos, SP, Brazil.*

PACS nos.: 42.25.Bs; 42.25.Fx; 41.20.Jb; 46.40.Cd. OCIS codes: 999.9999; 260.1960; 070.7545; 070.0070 200.0200; 050.1120; 070.1060; 280.0280; 050.1755. Keywords: wave equations; wave propagation; localized waves; non-diffracting waves (NDW); Bessel beams; Optics; Microwaves; Acoustics; totally forward NDW pulses; finite apertures; finite energies; functional expression for any NDW pulses; truncated waves; analytic description of truncated beams; subluminal NDWs; subluminal electromagnetic bullets; subsonic acoustic bullets; stationary solutions; zero-speed envelopes; "frozen waves" (FW); experimental production of FWs; Special relativity; Non-Restricted special Relativity; Lorentz transformations; electromagnetic X-shaped waves; acoustic X-shaped supersonic waves.

1 A General Introduction

1.1 A prologue

In this work, which essentially deals with *exact* solutions to the wave equations, we begin by introducing the topic of Non-Diffracting Waves (NDW), including some brief historical remarks, and by a simple definition of NDWs: Afterwards we present some recollections—besides of ordinary waves (gaussian beams, gaussian pulses)—of the simplest non-diffracting waves (Bessel beams, X-shaped pulses,...). More details can be found in the first two (introductory) chapters of the volume on *Localized Waves* published[1] by J.Wiley (Hoboken, NJ, USA) in 2008. In Section 2 we go on to show how to eliminate *any* backward-traveling components (also known as non-causal components), first in the case of ideal NDW pulses, and then, in Section 3, for realistic, finite-energy NDW pulses. In

^(†) Work partially supported by FAPESP, CAPES and CNPq (Brazil), and by INFN (Italy). E-mail addresses: recami@mi.infn.it, mzamboni@decom.fee.unicamp.br; hugo@decom.fee.unicamp.br; leo@sc.usp.br

particular, in subsection 3.1 we forward a general functional expression for any totally-forward non-diffracting pulses. Then, in Section 4 an efficient method is set forth for the *analytic* description of *truncated* beams, a byproduct of its being the elimination of any need of lengthy numerical calculations. In Section 5 we explore the not less interesting question of the *subluminal* NDWs, or bullets, in terms of two different methods, the second one being introduced since it allows the analytic description of $v = 0$ NDWs, that is, of non-diffracting waves with a static envelope (“Frozen Waves”, FW), in terms of continuous Bessel beam superpositions. The production of such Frozen Waves (which, indeed, have been experimentally generated in recent time for Optics) is theoretically developed in Section 6 also for the case of absorbing media. Section 7 discusses the role of Special Relativity and of Lorentz transformations, which is relevant for the physical comprehension of the whole issue of NDWs. In Section 8 we present further analytic solutions to the wave equations, with use of higher-order Bessel beams (namely, non-axially symmetric solutions). Next Section, 9, deals in detail with an application of NDWs to Biomedical Optics, by having recourse to the generalized Lorenz-Mie theory. In Section 10 we exploit the important fact that “soliton-like” solutions can be found also in the rather different case of the ordinary, linear *Schroedinger equation*—which is not a properly said wave-equation— within standard Quantum Mechanics; by constructing, for instance, also a general exact non-diffracting solution for such equation. These “localized” solutions to the Schroedinger equation may a priori be of help for a better understanding, say, of de Broglie’s approach and of the particle-wave duality. Some complementary issues are just mentioned in the last Section. The present work also constitutes a part of a much longer Review in preparation.

Let us now start by recalling that diffraction and dispersion are known since long to be phenomena limiting the applications of beams or pulses.

Diffraction is always present, affecting any waves that propagate in two or three-dimensional media. Pulses and beams are constituted by waves traveling along different directions, which produces a gradual *spatial* broadening. This effect is a limiting factor whenever a pulse is needed which maintains its transverse localization, like, e.g., in free space communications, image forming, optical lithography, electromagnetic tweezers, etcetera.

Dispersion acts on pulses propagating in material media, causing mainly a *temporal* broadening: An effect due to the variation of the refraction index with the frequency, so that each spectral component of the pulse possesses a different phase-velocity. This entails a gradual temporal widening, which constitutes a limiting factor when a pulse is needed which maintains its *time* width, like, e.g., in communication systems.

It has been important, therefore, to develop techniques able to reduce those phenomena. The *Non-diffracting Waves*, known also as Localized Waves, are indeed able to resist diffraction for a long distance. Today, non-diffracting waves are well-established both theoretically and experimentally, and are having innovative applications not only in vacuum, but also in material (linear or non-linear) media, showing to be able to resist

also dispersion. As we were mentioning, their potential applications are being intensively explored, always with surprising results, in fields like Acoustics, Microwaves, Optics, and are promising also in Mechanics, Geophysics[2], and even Elementary particle physics[3] and Gravitational Waves. One interesting acoustic application has been already obtained in high-resolution ultra-sound scanning of moving organs in the human body. We shall see that NDWs are suitable superpositions of Bessel beams. And worth noticing is that peculiar superposition of Bessel beams can be used to obtain “static” non-diffracting wave fields, with high transverse localization, and whose longitudinal intensity pattern can assume any desired shape within a chosen interval $0 \leq z \leq L$ of the propagation axis: Such waves with a *static* envelope [4, 5, 6, 1, 7], that we called “Frozen Waves” (FW), have been experimentally produced in recent times in the case of Optics, as reported elsewhere also in the Book whose introductory chapter (Chap.1) is constituted by this paper. Those Frozen Waves promise to have very important applications (even in the field of medicine, and of tumor curing[8])

To confine ourselves to electromagnetism, let us recall again the present-day studies on electromagnetic tweezers, optical (or acoustic) scalpels, optical guiding of atoms or (charged or neutral) corpuscles, optical lithography, optical (or acoustic) images, communications in free space, remote optical alignment, optical acceleration of charged corpuscles, and so on.

1.2 Preliminary, and historical, remarks

As we were saying, ordinary beams and pulses are superpositions of plane waves which travel in different directions; this causes diffraction, and consequently an increasing spatial broadening of the waves during propagation. Incidentally, we are here considering only propagating, that is, *non-evanescent*, waves.

Surprisingly, solutions to the wave equations however exist, which represent in homogeneous media beams and pulses able to resist the effects of diffraction for long distances. Such solutions are called Non-diffracting Waves (NDW), or Localized Waves (LW); even if a better name would be “Limited-diffractions Waves”[9, 10].

The theory of NDWs allows compensating also for effects like dispersion and attenuation. Indeed, in dispersing homogeneous media, it is possible to construct pulses that simultaneously resist the effects *of diffraction and of surface dispersion*. And, in absorbing homogeneous media, it is also possible to construct beams that resist the simultaneous effects *of diffraction and of attenuation*.

For earlier reviews about NDWs, we can refer the reader, for instance, to the first two chapters of the book[1], as well as Ref.[11], and references therein. There, the reader will find general and formal (simple) introductions to NDWs, with more details on the separate cases of beams and of pulses; as well as on the rather different characteristics of the Bessel and of the NDWs waves, with respect to (w.r.t) the Gaussian ones. The important properties of the former w.r.t. the latter ones can find application, as well-known and as stressed therein, in all fields in which an essential role is played by a

wave-equation (like electromagnetism, optics, acoustics, seismology, geophysics, and also gravitation, elementary particle physics, etc.).

Here, let us only insert the following, quite brief historical information:

The non-diffracting solutions to the wave equations (scalar, vectorial, spinorial,...) are in fashion, both in theory and in experiment, since a couple of decades. Rather well-known are the ones with luminal or superluminal peak-velocity[1]: Like the so-called X-shaped waves(see [9, 12, 13] and refs. therein), which are supersonic in Acoustics[10], and superluminal in Electromagnetism (see[14]; see also[15] and [16]).

By Bateman[17] and later on Courant & Hilbert[18], it had been already recognized that *luminal* NDWs exist, which are solutions to the wave equations. After the subsequent early works, already quoted by us, a great deal of results[19] has been published on NDWs, from both the theoretical and the experimental point of view: Initially, taking only free space into account; later on, considering more complex media which exhibit effects such as dispersion (see, e.g., [20, 21, 22]), nonlinearity[23], anisotropy[24, 25, 26], losses[5], and so on. Extensions of this type have been carried out along with the development, for instance, of efficient methods for obtaining non-diffracting beams and pulses in the subluminal, luminal and superluminal regimes, thus allowing easier experimental verifications.

Indeed, in recent years, some attention[19, 27, 28, 29, 30, 31, 32, 33, 34, 35] started to be paid to the (more “orthodox”) *subluminal* NDWs too. It should be stressed that, in any case, the interest of the NDWs resides not in their peak-velocity[36, 37, 38], but in the circumstance that they propagate in a homogeneous linear medium without distortion—and in a self-reconstructing way[39, 40, 5]— (apart from local variations: In the sense that their square magnitude keeps its shape during propagation, while local variations are shown only by its real, or imaginary, part).

In the past, however, much attention was not even paid to Brittingham’s 1983 paper[41], wherein he obtained *pulse-type* solutions to the Maxwell equations, which propagated in free space as a new kind of *c*-speed “solitons”. That lack of attention was partially due to the fact that Brittingham had been able neither to get finite-energy expressions for his “wavelets”, nor to make suggestions about their practical production. Two years later, however, Sezginer[42] was able to obtain quasi-nondiffracting luminal pulses endowed with a finite energy: Finite-energy pulses are known to travel no longer undistorted for an infinite distance, but nevertheless propagate without deformation for a long field-depth, much larger than the one achieved by ordinary pulses like the gaussian ones: Cf., e.g., Refs.[43, 44, 45, 46, 47, 48, 49, 50, 51, 52, 53, 54] and refs. therein.

An interesting problem, indeed, was that of investigating what it would happen to the ideal *Bessel beam solution when truncated* by a finite transverse aperture. In 1987 a heuristical answer came, after the quoted series of pioneering papers[43, 44, 45, 46], from the known experiment by Durnin et al.[47, 48], when it was shown that a realistic Bessel

beam, passing through a finite aperture, is able to travel keeping its transverse intensity shape approximately unchanged all along a *large* “depth of field”.

In any case, only after 1985 a general theory of NDWs started to be extensively developed[55, 56, 57, 9, 58, 59, 14, 60, 61, 62, 63, 12, 64, 65, 66, 67], both in the case of beams and in the case of pulses. For reviews, see for instance the Refs.[13, 63, 52, 53, 50, 54, 11, 1] and citations therein. For the propagation of NDWs in bounded regions (like *wave-guides*), see Refs.[68, 69, 70] and refs therein. For the focussing of NDWs, see e.g. Refs.[71, 72, 1] and quotations therein. For recourse to chirped optical X-type waves to obtain pulses capable of recovering their spatial shape both transversally and longitudinally, see e.g. Refs.[73, 1] and references therein. Not less important, as to the construction of general NDWs propagating in *dispersive* media, see, besides the quoted [20, 21, 22], also Refs.[74, 75, 76]; while, for *lossy* media, cf. both Ref.[5] and refs. therein, and this Chapter. At last, for finite-energy, or truncated, solutions see, e.g., Refs.[77, 78, 59, 79, 80, 81], as well as this Chapter.

By now, the NDWs have been experimentally produced[10, 82, 83, 84, 85], and are being applied in fields ranging from ultrasound scanning[86, 87, 30, 33] to optics (for the production, e.g., of new type of tweezers[8, 88, 5, 89, 90]). All those works have demonstrated that non-diffracting pulses can travel with any arbitrary peak-velocities v , that is, with speed v in the range $0 < v < \infty$.

Let us introduce at this point a first mathematical definition of NDWs:

Diffraction, as a spatial transverse spreading, cannot occur in the simple case of 1 space dimension. Actually, the 1D wave equation

$$(\partial_z^2 - 1/c^2 \partial_t^2)\psi(z, t) = 0 \tag{1}$$

admits the general solution $\psi = f(z - ct) + g(z + ct)$, quantities f and g being arbitrary (differentiable) functions; and, for instance, a solution of the type $\psi(z - ct)$ travels rigidly along the positive z -direction with speed c . Let us here recall, and stress, that, if a wave depends on t and z only through the quantity $z - Vt$, it will be seen as moving without any distortion with the speed V : See, e.g., Ref.[13] and references therein.

Passing on to the 3D case, when the wave equation reads

$$(\nabla_{\perp}^2 + \partial_z^2 - 1/c^2 \partial_t^2)\psi(\mathbf{r}_{\perp}, z, t) = 0, \tag{2}$$

quantity ∇_{\perp}^2 being the transverse Laplacian, and \mathbf{r}_{\perp} the transverse position vector [so that $\mathbf{r} = \mathbf{r}_{\perp} + z\mathbf{k}$], it is natural to look for possible solutions of the type

$$\psi(\mathbf{r}_{\perp}, z - Vt), \tag{3}$$

which would correspond to waves rigidly propagating along z with speed V , whatever be the value of V (cf. Refs.[1, 13]). To check the mentioned possibility, let us go back to

Eq.(90). It is simple to show, then, that an acceptable solution of the type (3) has just to satisfy the equation

$$(\nabla_{\perp}^2 + (1 - V^2/c^2)\partial_{\zeta}^2)\psi(\mathbf{r}_{\perp}, \zeta) = 0 , \quad (4)$$

where $\zeta \equiv z - Vt$. [Let us explicitly recall[52] that the shape of any solutions that depend on z and on t only through the quantity $z - Vt$ will always appear the same to an observer traveling along z with the speed V , whatever it be (subluminal, luminal or Superluminal) the value of V : That is, such a solution will propagate rigidly with speed V].

One can therefore realize that:

(i) when $V = c$, equation (4) becomes elliptic: Namely, it becomes a Laplace equation in the transverse variables, that prevents the free-space solution from being transversally localizable. In other words, these solutions are plane waves, or plane wave pulses, with scars practical interest.

(ii) when $V < c$, equation (4) is still elliptic: More specifically, it is a Laplace equation in the variables $(x, y, \zeta\sqrt{1 - V^2/c^2})$, so that the free-space solutions cannot admit any local maxima or minima. No solutions of physical interest are obtainable.

(iii) when $V > c$, however, equation (4) is hyperbolic, and it becomes possible to obtain non-diffracting solutions of the type $\psi(\mathbf{r}_{\perp}, z - Vt)$, both for beams and for pulses.

The latter simple and interesting result shows that, when basing ourselves on Eq.(4), the solutions that can propagate rigidly (that is, without any spatial modifications) are those corresponding to $V > c$. In the case of beams, V is merely the phase velocity; but in the case of pulses it is the peak velocity (sometimes identified with the group-velocity). Incidentally, it is known that, when one superposes waves whose phase-velocity does not depend on their frequency, such a phase-velocity becomes* the actual peak-velocity[69, 52, 91].

Many interesting solutions of this kind exist[1, 9, 10, 59, 14], and some of them will be mentioned in this Chapter, and in the related 2014 Book. From the historical point of view, let us repeat that such solutions to the wave equations (and, in particular, to the Maxwell equations, under weak hypotheses) were theoretically predicted long time ago[92, 93, 18, 17], mathematically constructed in more recent times[9, 14, 94], and soon after experimentally produced[10, 82, 83, 85].

However, *it is rather restrictive to define a NDW as a solution of the type (3), with $V > c$* . Actually, also *subluminal* NDW solutions to the wave equations exist[19], and they too are rather interesting, as we shall discuss below.

*Let us here recall that the group velocity can be written as $\mathbf{v}_g = \nabla_k \omega = \partial\omega/\partial k_z \mathbf{z}$ only when k_x and k_y remain (almost) constant in the considered superposition, as it happens e.g. in the case of metallic guides.

1.3 Definition of Non-diffracting Wave (NDW)

Therefore, it is convenient to formulate a *more comprehensive* definition, wherefrom to derive a much ampler set of solutions (super-luminal, luminal, or sub-luminal) capable of withstanding diffraction: Both for infinite distances, in the ideal case (of infinite energy), and for large but finite distances, in the realistic case (of finite energy).

Let us start by formulating an adequate definition of an *ideal* Non-diffracting Wave.

Let us consider a linear and homogeneous wave equation in free space. In cylindrical coordinates (ρ, ϕ, z) and using a Fourier-Bessel expansion, its general solution $\psi(\rho, \phi, z, t)$ can be expressed, when disregarding evanescent waves, as

$$\Psi(\rho, \phi, z, t) = \sum_{n=-\infty}^{\infty} \left[\int_0^{\infty} dk_{\rho} \int_{-\infty}^{\infty} dk_z \int_{-\infty}^{\infty} d\omega k_{\rho} A'_n(k_{\rho}, k_z, \omega) J_n(k_{\rho}\rho) e^{ik_z z} e^{-i\omega t} e^{in\phi} \right] \quad (5)$$

with

$$A'_n(k_{\rho}, k_z, \omega) = A_n(k_z, \omega) \delta \left[k_{\rho}^2 - \left(\frac{\omega^2}{c^2} - k_z^2 \right) \right], \quad (6)$$

the $A_n(k_z, \omega)$ being arbitrary functions, and $\delta(\cdot)$ the Dirac delta function. It is important to emphasize that the $J_n(k_{\rho}\rho)$ are n -order *Bessel functions*. For simplicity, many authors often confined themselves to the zero-order Bessel functions $J_0(\cdot)$.

An ideal NDW is a wave that must be capable of maintaining indefinitely its spatial form (except for local variations) while propagating. This property may be mathematically expressed, when assuming propagation in the z direction, as follows:

$$\Psi(\rho, \phi, z, t) = \Psi \left(\rho, \phi, z + \Delta z_0, t + \frac{\Delta z_0}{V} \right), \quad (7)$$

where Δz_0 is a chosen length, and V is the pulse-peak velocity, with $0 \leq V \leq \infty$. Then, by using Eq.(5) into Eq.(7), and taking account of Eq.(6), one can show[65, 1, 12] that any non-diffracting solution can be written

$$\begin{aligned} \Psi(\rho, \phi, z, t) = & \sum_{n=-\infty}^{\infty} \sum_{m=-\infty}^{\infty} \left[\int_{-\infty}^{\infty} d\omega \int_{-\omega/c}^{\omega/c} dk_z A_{nm}(k_z, \omega) \right. \\ & \left. \times J_n \left(\rho \sqrt{\frac{\omega^2}{c^2} - k_z^2} \right) e^{ik_z z} e^{-i\omega t} e^{in\phi} \right] \end{aligned} \quad (8)$$

with

$$A_{nm}(k_z, \omega) = S_{nm}(\omega) \delta(\omega - (Vk_z + b_m)), \quad (9)$$

it being $b_m = 2m\pi V/\Delta z_0$ (with m an integer number too, of course), while quantity $S_{nm}(\omega)$ is an arbitrary *frequency spectrum*. Notice that, due to Eq.(9), each term in the double sum (8), namely in its expression within square brackets, is a truly non-diffracting

wave (beam or pulse); and their sum (8) is just the most general form representing *an ideal NDW* according to definition (7).

One should also notice that (8) *is nothing but a superposition of Bessel beams* with a specific “space-time coupling”, characterized by *linear relationships* between their angular frequency ω and their longitudinal wave number k_z .

Concerning such a superposition, the Bessel beams with $\omega/k_z > 0$ ($\omega/k_z < 0$) propagate in the positive (negative) z direction. As we wish to obtain NDWs propagating in the positive z direction, it is not desirable the presence of “backward” Bessel beams, i.e. of “backward components” —often called *non-causal*, since they should be *entering* the antenna or generator—. The problems with the backward-moving components, that so frequently plague the localized waves, can be however overcome by appropriate choices of the spectrum (9), which can totally eliminate those components, or minimize their contribution, in superposition (8). Let us notice that often only positive values of ω are considered ($0 \leq \omega \leq \infty$).

Another important point refers to the energy[42, 54, 95, 12] of the NDWs. It is well known that any ideal NDW, i.e., any field with the spectrum (9), possesses infinite energy. However finite-energy NDWs can be constructed by concentrating the spectrum $A_{nm}(k_z, \omega)$ in the surrounding of a straight line of the type $\omega = V k_z + b_m$ instead of collapsing it exactly over that line[12, 65]. In such a case, the NDWs get a finite energy, but, as we know, are endowed with *finite* field depths: i.e., they maintain their spatial forms for long (but not infinite) distances.

Despite the fact that expression (8), with $A_{nm}(k_z, \omega)$ given by (9), does represent ideal non-diffracting waves, it is difficult to use it for obtaining analytical solutions, especially when having the task of eliminating the backward components. This difficulty becomes even worse in the case of finite-energy NDWs. We shall come back to this point in Section 2.

1.4 First examples

Before going on, let us be more concrete. First of all, let us notice that Eq.(5), for $n = 0$ and on integrating over k_z , reduces to the less general —but still quite useful— solution

$$\psi(\rho, z, t) = \int_{-\infty}^{\infty} \int_0^{\omega/ck_\rho} J_0(k_\rho \rho) e^{i\sqrt{\omega^2/c^2 - k_\rho^2} z} e^{-i\omega t} S(k_\rho, \omega) dk_\rho d\omega \quad (10)$$

where $S(k_\rho, \omega)$ is now the chosen spectral function, with only $k_z > 0$ (and we still disregard evanescent waves). We are using the standard relation

$$\frac{\omega^2}{c^2} = k_\rho^2 + k_z^2 . \quad (11)$$

From the integral solution (10) one can get in particular, for instance, the (**non-localized**) gaussian beams and pulses, to which we shall refer for illustrating the differences of the NDWs with respect to them.

The Gaussian Beam — A very common (non-localized) beam is the gaussian beam[96], corresponding to the spectrum

$$S(k_\rho, \omega) = 2a^2 e^{-a^2 k_\rho^2} \delta(\omega - \omega_0) . \quad (12)$$

In Eq.(12), a is a positive constant, which will be shown to depend on the transverse aperture of the initial pulse.

The integral solution (10), with spectral function (12), can be regarded as a *superposition* of plane waves: Namely, *of plane waves propagating in all directions (always with $k_z \geq 0$), the most intense ones being those directed along (positive) z* [especially when $\Delta k_\rho \equiv 1/a \ll \omega_0/c$]. This is clearly depicted in Fig.1.4 of [1].

On substituting Eq.(12) into Eq.(10) and adopting the paraxial approximation [which is known to be just valid if $\Delta k_\rho \equiv 1/a \ll \omega_0/c$], one meets the gaussian beam

$$\psi_{\text{gauss}}(\rho, z, t) = \frac{a^2 \exp\left(\frac{-\rho^2}{4(a^2 + iz/2k_0)}\right)}{(a^2 + iz/2k_0)} e^{ik_0(z-ct)} , \quad (13)$$

where $k_0 = \omega_0/c$. We can verify that the magnitude $|\psi|$ of such a beam, which suffers transverse diffraction, doubles its initial width $\Delta\rho_0 = 2a$ after having traveled the distance $z_{\text{dif}} = \sqrt{3} k_0 \Delta\rho_0^2/2$, called diffraction length. The more concentrated a gaussian beam happens to be, the more rapidly it gets spoiled.

The Gaussian Pulse — The most common (non-localized) *pulse* is the gaussian pulse, which is got from Eq.(10) by using the spectrum[73]

$$S(k_\rho, \omega) = \frac{2ba^2}{\sqrt{\pi}} e^{-a^2 k_\rho^2} e^{-b^2(\omega-\omega_0)^2} \quad (14)$$

where a and b are positive constants. Indeed, such a pulse is a superposition of gaussian beams of different frequency.

Now, on substituting Eq.(14) into Eq.(10), and adopting once more the paraxial approximation, one gets the gaussian pulse:

$$\psi(\rho, z, t) = \frac{a^2 \exp\left(\frac{-\rho^2}{4(a^2 + iz/2k_0)}\right) \exp\left(\frac{-(z-ct)^2}{4c^2 b^2}\right)}{a^2 + iz/2k_0} , \quad (15)$$

endowed with speed c and temporal width $\Delta t = 2b$, and suffering a progressing enlargement of its transverse width, so that its initial value gets doubled already at position $z_{\text{dif}} = \sqrt{3} k_0 \Delta\rho_0^2/2$, with $\Delta\rho_0 = 2a$. Let us remind that the paraxial approximation is really valid in the pulse case only if there hold the two conditions $\Delta k_\rho \equiv 1/a \ll \omega_0/c$, and $\Delta\omega = 1/b \ll \omega_0$, imposing a slow variation of the envelope.

1.5 Further examples: The Non-diffracting Solutions

Let us finally go on to the construction of the two most renowned localized waves[50]: the Bessel beam, and the ordinary X-shaped pulse. First of all, let us recall that, when superposing (axially symmetric) solutions of the wave equation in the vacuum, three spectral parameters, (ω, k_ρ, k_z) , come into the play, which have however to satisfy the constraint (11), deriving from the wave equation itself. Consequently, only two of them are independent: and we choose here ω and k_ρ . Such a possibility of choosing ω and k_ρ was already apparent in the spectral functions generating gaussian beams and pulses, which consisted in the product of two functions, one depending only on ω and the other on k_ρ .

We are going to see that further particular relations between ω and k_ρ [or, analogously, between ω and k_z] can be moreover enforced, in order to get interesting and unexpected results, such as the *non-diffracting waves*.

The Bessel beam — Let us start by imposing a *linear* coupling between ω and k_ρ (it could be actually shown[48] that it is the unique coupling leading to NDW solutions).

Namely, let us consider the spectral function

$$S(k_\rho, \omega) = \frac{\delta(k_\rho - \frac{\omega}{c} \sin \theta)}{k_\rho} \delta(\omega - \omega_0) , \quad (16)$$

which implies that $k_\rho = (\omega \sin \theta)/c$, with $0 \leq \theta \leq \pi/2$: A relation that can be regarded as a space-time coupling. Let us add that this linear constraint between ω and k_ρ , together with relation (11), yields $k_z = (\omega \cos \theta)/c$. This is an important fact, since an *ideal* non-diffracting wave *must* contain[50, 12] a coupling of the type $\omega = V k_z + b$, where V and b are arbitrary constants. The integral function (10), this time with spectrum (16), can be interpreted as a superposition of plane waves too: But this time the axially-symmetric Bessel beam appears as the result of the *superposition of plane waves whose wave vectors lay on the surface of a cone having the propagation line as its symmetry axis and an opening angle equal to θ* ; such θ being called the *axicon angle*. This is clearly shown in Fig.1.5 of [1].

By inserting Eq.(16) into Eq.(10), one gets the mathematical expression of the so-called *Bessel beam*:

$$\psi(\rho, z, t) = J_0 \left(\frac{\omega_0}{c} \sin \theta \rho \right) \exp \left[i \frac{\omega_0}{c} \cos \theta \left(z - \frac{c}{\cos \theta} t \right) \right] . \quad (17)$$

This beam possesses phase-velocity $v_{\text{ph}} = c/\cos \theta$, and field transverse shape represented by a Bessel function $J_0(\cdot)$ so that its field is concentrated in the surroundings of the propagation axis z . Moreover, Eq.(17) tells us that the Bessel beam keeps its transverse shape (which is therefore invariant) while propagating, with central “spot” $\Delta \rho = 2.405c/(\omega \sin \theta)$.

The ideal Bessel beam, however, is not square-integrable in the transverse direction, and is therefore associated with an infinite power flux: i.e., it cannot be experimentally produced. One must have recourse to truncated Bessel beams, generated by finite apertures: In this case the (truncated) Bessel beams are still able to travel a long distance while maintaining their transfer shape, as well as their speed, approximately unchanged[47, 48, 97, 98]. For instance, the field-depth of a Bessel beam generated by a circular finite aperture with radius R is given [if $R \gg \Delta\rho_0 = 2.4/k_\rho$] by

$$Z_{\max} = \frac{R}{\tan \theta}, \quad (18)$$

where θ is the beam axicon angle. In the finite aperture case, the Bessel beam cannot be represented any longer by Eq.(17), and one must calculate it by the scalar diffraction theory: by using, for example, Kirchhoff's or Rayleigh-Sommerfeld's diffraction integrals. But till the distance Z_{\max} one may still use Eq.(17) for approximately describing the beam, at least in the vicinity of the axis $\rho = 0$, that is, for $\rho \ll R$. To realize how much a truncated Bessel beam succeeds in resisting diffraction, one can consider also a gaussian beam, with the same frequency and central "spot", and *compare* their field-depths. In particular, let both the beams have $\lambda = 0.63 \mu\text{m}$ and initial central "spot" size $\Delta\rho_0 = 60 \mu\text{m}$. The Bessel beam will possess axicon angle $\theta = \arcsin[2.405c/(\omega\Delta\rho_0)] = 0.004 \text{ rad}$. In the case, e.g., of a circular aperture with radius 3.5 mm, it is then easy to verify that the gaussian beam doubles its initial transverse width already after 3 cm, while after 6 cm its intensity has become an order of magnitude smaller. By contrast, the truncated Bessel beam keeps its transverse shape until the distance $Z_{\max} = R/\tan\theta = 85 \text{ cm}$. Afterwards, the Bessel beam rapidly decays, as a consequence of the sharp cut performed on its aperture (such cut being responsible also for some intensity oscillations suffered by the beam along its propagation axis, and for the fact that the feeding waves, coming from the aperture, at a certain point get eventually faint). All this is clearly depicted in Fig.1.6 of [1].

It may be useful to repeat that a Bessel beam is characterized by an "extended focus" along its propagation axis, so that its energy cannot be concentrated inside a small region in the transverse plane: It needs, on the contrary, to be continuously reconstructed by the energy associated with the "lateral rings" (evolving along closing conical surfaces) which constitute its transverse structure. This is quite different from the case of a Gaussian beam, which possesses a point-like focus: That is, it is constructed so as to concentrate its energy within a spot that becomes very small at a certain point of its propagation axis, and afterwards rapidly diffracts.

The zeroth-order (axially symmetric) Bessel beam is nothing but one example of localized beam. Further examples are the higher order (not cylindrically symmetric) Bessel beams, described by Eq.(1.13) of [1], or the Mathieu beams[51], and so on.

The Ordinary X-shaped Pulse — Following the same procedure adopted in the previous

subsection, let us construct pulses by using spectral functions of the type

$$S(k_\rho, \omega) = \frac{\delta(k_\rho - \frac{\omega}{c} \sin \theta)}{k_\rho} F(\omega), \quad (19)$$

where this time the Dirac delta function furnishes the spectral space-time coupling $k_\rho = (\omega \sin \theta)/c$. Function $F(\omega)$ is, of course, the frequency spectrum; it is left for the moment undetermined. On using Eq.(19) into Eq.(10), one obtains

$$\psi(\rho, z, t) = \int_{-\infty}^{\infty} F(\omega) J_0\left(\frac{\omega}{c} \sin \theta \rho\right) \exp\left(\frac{\omega}{c} \cos \theta \left(z - \frac{c}{\cos \theta} t\right)\right) d\omega. \quad (20)$$

It is easy to see that ψ will be a pulse of the type

$$\psi = \psi(\rho, z - Vt) \quad (21)$$

with a speed $V = c/\cos \theta$ independent of the frequency spectrum $F(\omega)$.

Such solutions are known as X-shaped pulses, and are (*non-diffracting*) waves in the sense that they do obviously maintain their spatial shape during propagation (see., e.g., Refs.[9, 14, 12] and refs. therein; as well as the following). Their peak velocity is well-known to be superluminal (cf.also Refs.[37, 36, 99] and refs therein). Some relevant, useful comments have been added, for instance, at pages 12-13 of [1].

Now, let us for instance consider in Eq.(20) the particular frequency spectrum $F(\omega)$ given by

$$F(\omega) = H(\omega) \frac{a}{V} \exp\left(-\frac{a}{V} \omega\right), \quad (22)$$

where $H(\omega)$ is the Heaviside step-function and a a positive constant. Then, Eq.(20) yields

$$\psi(\rho, \zeta) \equiv X = \frac{a}{\sqrt{(a - i\zeta)^2 + \left(\frac{V^2}{c^2} - 1\right) \rho^2}}, \quad (23)$$

still with $\zeta \equiv z - Vt$. This solution (23) is the well-known ordinary, or “classic”, X-wave, which constitutes a simple example of a superluminal [supersonic, in the case of Acoustics] X-shaped pulse.[9, 14] Notice that function (22) contains mainly low frequencies, so that the classic X-wave is suitable for low frequencies only.

Actually, Lu et al. first introduced them for Acoustic. Soon after having mathematically and experimentally constructed their “classic” (acoustic) X-wave, they started applying them to ultrasonic scanning, directly obtaining very high quality 3D images. Subsequently, in 1996 there were mathematically constructed (see, e.g., Ref.[14] and refs. therein) the analogous X-shaped solutions to the Maxwell equations, by working out scalar superluminal non-diffracting solutions for each component of the Hertz potential. In reality, Ziolkowski et al.[59] had already found in electromagnetism similar solutions for the simple scalar case, called by them *slingshot* pulses; but their pioneering solutions

had gone almost unnoticed at that time (1993). In 1997 Saari et al.[82] announced the first production of an X-shaped wave in the optical realm, thus proving experimentally the existence of superluminal non-diffracting electromagnetic pulses. Let us add that X-shaped waves have been easily produced also in nonlinear media[23].

Figure 23 depicts (the real part of) an ordinary X-wave with $V = 1.1 c$ and $a = 3$ m.

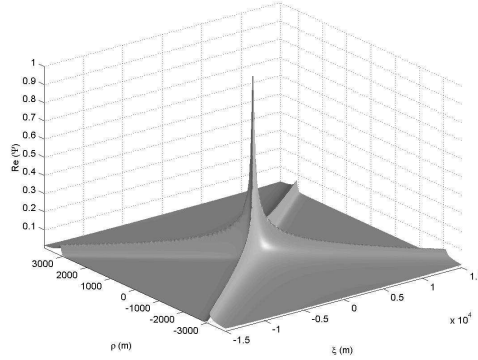


Figure 1: Plot of the real part of the ordinary X-wave, evaluated for $V = 1.1 c$ with $a = 3$ m .

Solutions (20), and in particular the pulse (23), have got an infinite field-depth, and an infinite energy as well. Therefore, as it was mentioned in the Bessel beam case, one should pass to truncated pulses, originating from a finite aperture. Afterwards, our truncated pulses will keep their spatial shape (and their speed) all along the depth of field

$$Z = \frac{R}{\tan \theta}, \quad (24)$$

where, as before, R is the aperture radius and θ the axicon angle (and R is assumed to be much larger than the X-pulse spot).

At this point, it is worthwhile to add Fig.2, with its detailed caption.

For further X-type solutions, with less and less energy distributed along their “arms”, let us refer the reader to papers like [12, 65] and references therein, as well as to [1]. For example, it was therein addressed the explicit construction of infinite families of generalizations of the classic X-shaped wave, with energy more and more concentrated around their vertex: Cf., e.g., Figs.1.9 in [1]). Elsewhere, the techniques have been found for building up new series of non-diffracting superluminal solutions to the Maxwell equations suitable for arbitrary frequencies and bandwidths; and so on.

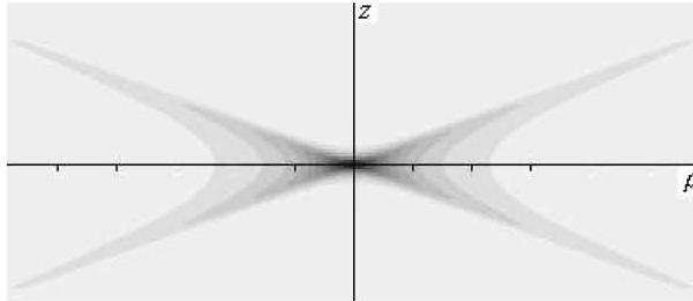


Figure 2: All the X-waves (truncated or not) must have a leading cone in addition to the rear cone, such a leading cone having a role even for the peak stability[9]. Long ago, this was also predicted, in a sense, by (non-restricted[13, 14, 1]) special relativity: one should not forget, in fact, that *all* wave-equations, and not only Maxwell’s, have an intrinsic relativistic structure... By contrast, the fact that X-waves have a conic shape induced some authors to look for (untenable) links —let us now confine ourselves to electromagnetism— between them and the Cherenkov radiation, so as to deny the existence of the leading cone: But X-shaped waves have nothing to do with Cherenkov!, as it has been thoroughly demonstrated in Refs.[36, 37, 99]. In practice, when wishing to produce concretely a finite conic non-diffracting wave, truncated both in space and in time, one is supposed to have recourse *in the simplest case* to a dynamic antenna emitting a radiation cylindrically symmetric in space and symmetric in time).[1]

2 Eliminating any Backward Components: Totally Forward NDW Pulses

As we mentioned, Eq.(8), with its $A_{nm}(k_z, \omega)$ given by (9), even if representing ideal solutions, is difficult to be used for obtaining analytical solutions with elimination of the “non-causal” components; a difficulty which becomes worse in the case of finite-energy NDWs. As promised, let us come back to these problems putting forth a method[65] for getting exact NDW solutions *totally free of backward components*.

Let us start with Eqs.(5,6), which describe a general free-space solution (without evanescent waves) of the homogeneous wave equation, and consider in Eq.(6) a spectrum $A_n(k_z, \omega)$ of the type

$$A_n(k_z, \omega) = \delta_{n0}H(\omega)H(k_z)A(k_z, \omega) \quad (25)$$

where δ_{n0} is the Kronecker delta function, $H(\cdot)$ the Heaviside function and $\delta(\cdot)$ the Dirac delta function, quantity $A(k_z, \omega)$ being an arbitrary function. Spectra of the type (25) restrict the solutions to the axially symmetric case, with only positive values to the angular frequencies and longitudinal wave numbers. With this, the solutions proposed by us get

the integral form

$$\psi(\rho, z, t) = \int_0^\infty d\omega \int_0^{\omega/c} dk_z A(k_z, \omega) J_0(\rho\sqrt{\omega^2/c^2 - k_z^2}) e^{ik_z z} e^{-i\omega t}, \quad (26)$$

that is, they result to be general superpositions of zero-order Bessel beams propagating in the positive z direction only. Therefore, any solution obtained from (26), be they non-diffracting or not, are *completely free* from backward components.

At this point, we can introduce the *unidirectional* decomposition

$$\begin{cases} \zeta = z - Vt \\ \eta = z - ct \end{cases} \quad (27)$$

with $V > c$.

A decomposition of this type has been used till now in the context of paraxial approximation only[100, 101]; but we are going to show that it can be much more effective, giving important results in the context of exact solutions, and in situations that cannot be analyzed in the paraxial approach.

With (27), we can write the integral solution (26) as

$$\psi(\rho, \zeta, \eta) = (V - c) \int_0^\infty d\sigma \int_{-\infty}^\sigma d\alpha A(\alpha, \sigma) J_0(\rho\sqrt{\gamma^{-2}\sigma^2 - 2(\beta - 1)\sigma\alpha}) e^{-i\alpha\eta} e^{i\sigma\zeta} \quad (28)$$

where $\gamma = (\beta^2 - 1)^{-1/2}$, $\beta = V/c$ and where

$$\begin{cases} \alpha = \frac{1}{V - c} (\omega - V k_z) \\ \sigma = \frac{1}{V - c} (\omega - c k_z) \end{cases} \quad (29)$$

are the new spectral parameters.

It should be stressed that superposition (28) is not restricted to NDWs: It is the choice of the spectrum $A(\alpha, \sigma)$ that will determine the resulting NDWs.

2.1 Totally forward ideal superluminal NDW pulses

The X-type waves. The most trivial NDW solutions are the X-type waves. We have seen that they are constructed by frequency superpositions of Bessel beams with the same phase velocity $V > c$ and *till now* constitute the only known ideal NDW pulses free of backward components. It is not necessary, therefore, to use the present method to obtain such X-type waves, since they can be obtained by using directly the integral representation in the parameters (k_z, ω) , i.e., by using Eq.(26). Even so, let us use our new approach to construct the ordinary X wave.

Consider the spectral function $A(\alpha, \sigma)$ given by

$$A(\alpha, \sigma) = \frac{1}{V - c} \delta(\alpha) e^{-s\sigma} \quad (30)$$

One can notice that the delta function in (30) implies that $\alpha = 0 \rightarrow \omega = V k_z$, which is just the spectral characteristic of the X-type waves. In this way, the exponential function $\exp(-s\sigma)$ represents a frequency spectrum starting at $\omega = 0$, with an exponential decay and frequency bandwidth $\Delta\omega = V/s$.

Using (30) in (28), we get

$$\psi(\rho, \zeta) = \frac{1}{\sqrt{(s - i\zeta)^2 + \gamma^{-2}\rho^2}} \equiv X \quad , \quad (31)$$

which is the well known ordinary X wave.

Totally forward Superluminal Focus Wave Modes. Focus wave modes (FWM) [56, 54, 12] are ideal non-diffracting pulses possessing spectra with a constraint of the type $\omega = \mathcal{V}k_z + b$ (with $b \neq 0$), which links the angular frequency with the longitudinal wave number, and are known for their strong field concentrations.

Till now, all the known FWM solutions possessed, however, backward spectral components, a fact that, as we know, forces one to consider large frequency bandwidths to minimize their contribution. However we are going to obtain solutions of this type completely free of backward components, and able to possess also very narrow frequency bandwidths.

Let us choose a spectral function $A(\alpha, \sigma)$ like

$$A(\alpha, \sigma) = \frac{1}{V - c} \delta(\alpha + \alpha_0) e^{-s\sigma} \quad (32)$$

with $\alpha_0 > 0$ a constant. This choice confines the spectral parameters ω, k_z of the Bessel beams to the straight line $\omega = V k_z - (V - c)\alpha_0$, as it is shown in figure 3 below

Substituting (32) in (28), we have

$$\psi(\rho, \zeta, \eta) = \int_0^\infty d\sigma \int_{-\infty}^\sigma d\alpha \delta(\alpha + \alpha_0) e^{-s\sigma} J_0(\rho \sqrt{\gamma^{-2}\sigma^2 - 2(\beta - 1)\sigma\alpha}) e^{-i\alpha\eta} e^{i\sigma\zeta} \quad , \quad (33)$$

which, on using identity 6.616 in Ref.[102], results in

$$\psi(\rho, \zeta, \eta) = X e^{i\alpha_0\eta} \exp \left[\frac{\alpha_0}{\beta + 1} (s - i\zeta - X^{-1}) \right] \quad (34)$$

where X is the ordinary X-wave given by Eq.(31).

Solution (34) represents an ideal superluminal NDW of the type FWM, but totally free from backward components.

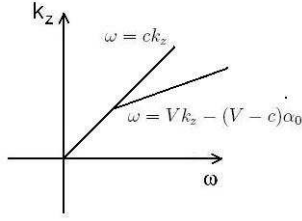


Figure 3: The Dirac delta function in (32) confines the spectral parameters ω, k_z of the Bessel beams to the straight line $\omega = Vk_z - (V - c)\alpha_0$, with $\alpha_0 > 0$.

As we already said, the Bessel beams constituting this solution have their spectral parameters linked by the relation $\omega = Vk_z - (V - c)\alpha_0$; thus, by using (32) and (29), it is easy to see that the frequency spectrum of those Bessel beams starts at $\omega_{\min} = c\alpha_0$ with an exponential decay $\exp(-s\omega/V)$, and so possesses the bandwidth $\Delta\omega = V/s$. It is clear that ω_{\min} and $\Delta\omega$ can assume any values, so that the resulting FWM, Eq.(34), can range from a quasi-monochromatic to an ultrashort pulse. This is a great advantage with respect to the old FWM solutions.

As an example, we plot in figure 4 one case related with the NDW pulse given by Eq.(34).

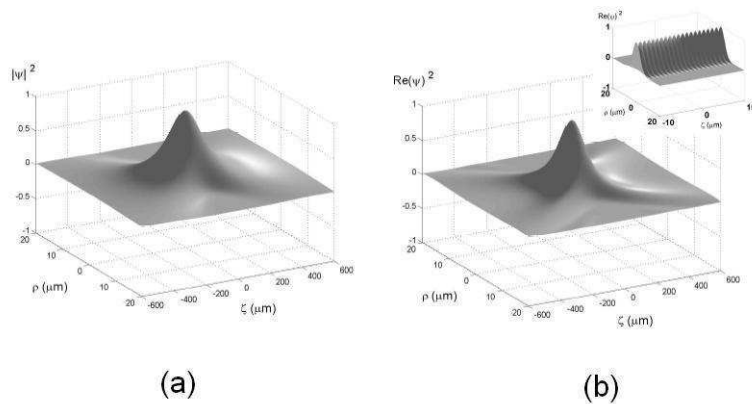


Figure 4: **(a)** and **(b)** show, respectively, the intensity of the complex and real part of a quasi-monochromatic, totally “forward”, superluminal FWM optical pulse, with $V = 1.5c$, $\alpha_0 = 1.256 \times 10^7 \text{ m}^{-1}$ and $s = 1.194 \times 10^{-4} \text{ m}$, which correspond to $\omega_{\min} = 3.77 \times 10^{15} \text{ Hz}$, and $\Delta\omega = 3.77 \times 10^{12} \text{ Hz}$, i.e., to a picosecond pulse with $\lambda_0 = 0.5 \mu\text{m}$.

In Figs.(4) we have a quasi-monochromatic optical FWM pulse, with $V = 1.5c$, $\alpha_0 = 1.256 \times 10^7 \text{ m}^{-1}$ and $s = 1.194 \times 10^{-4} \text{ m}$, which correspond to $\omega_{\min} = 3.77 \times 10^{15} \text{ Hz}$, and $\Delta\omega = 3.77 \times 10^{12} \text{ Hz}$, i.e., to a picosecond pulse with $\lambda_0 = 0.5 \mu\text{m}$. Figure (4a) shows

the intensity of the complex NDW field, while Fig.4b shows the intensity of its real part. Moreover, in Fig.4b, in the right upper corner, it is shown a zoom of this NDW, on the z axis and around the pulse's peak, where the carrier wave of this quasi-monochromatic pulse shows up.

Now, we apply our method to obtain totally forward *finite-energy* NDW pulses.

3 Totally Forward, *Finite-Energy* NDW Pulses

Finite-energy NDW pulses are *almost* non-diffracting, in the sense that they can retain their spatial forms, resisting to the diffraction effects, for long (but not infinite) distances.

There exist many analytical solutions representing finite-energy NDWs[56, 54, 12], but, once more, all the known solutions suffer from the presence of backward components. We can overcome this limitation.

We are going on skipping here the subluminal NDWs, which will be addressed below in Section 5, where also the particularly interesting case of the NDSs “at rest” (Frozen Waves) will be briefly considered.

Superluminal finite-energy NDW pulses, with peak velocity $V > c$, can be got by choosing spectral functions in (26) which are concentrated in the vicinity of the straight line $\omega = Vk_z + b$ instead of lying on it. Similarly, in the case of luminal finite-energy NDW pulses the spectral functions in (26) have to be concentrated in the vicinity of the straight line $\omega = ck_z + b$ (note that in the luminal case, one must have $b \geq 0$).

Indeed, from Eq.(29) it is easy to see that, by our approach, finite-energy superluminal NDWs can be actually obtained by concentrating the spectral function $A(\alpha, \sigma)$ entering in (28), in the vicinity of $\alpha = -\alpha_0$, with α_0 a *positive* constant. And, analogously, the finite-energy luminal case can be obtained with a spectrum $A(\alpha, \sigma)$ concentrated in the vicinity of $\sigma = \sigma_0$, with $\sigma_0 \geq 0$.

To see this, let us consider the spectrum

$$A(\alpha, \sigma) = \frac{1}{V - c} H(-\alpha - \alpha_0) e^{a\alpha} e^{-s\sigma} \quad (35)$$

where $\alpha_0 > 0$, $a > 0$ and $s > 0$ are constants, and $H(\cdot)$ is the Heaviside function.

Due to the presence of the Heaviside function, the spectrum (35), when written in terms of the spectral parameters ω and k_z , has its domain in the region shown in Fig.5 below.

We can see that the spectrum $A(\alpha, \sigma)$ given by Eq.(35) is more concentrated on the line $\alpha = \alpha_0$, i.e, around $\omega = Vk_z - (V - c)\alpha_0$, or on $\sigma = 0$ (i.e., around $\omega = ck_z$), depending on the values of a and s : More specifically, the resulting solution will be a superluminal finite-energy NDW pulse, with peak velocity $V > c$, if $a \gg s$; or a luminal finite-energy NDW pulse if $s \gg a$.

Inserting the spectrum (35) into (28), we have

$$\psi(\rho, \zeta, \eta) = \int_0^\infty d\sigma \int_{-\infty}^{-\alpha_0} d\alpha e^{a\alpha} e^{-s\sigma} J_0(\rho \sqrt{\gamma^{-2}\sigma^2 - 2(\beta - 1)\sigma\alpha}) e^{-i\alpha\eta} e^{i\sigma\zeta} , \quad (36)$$

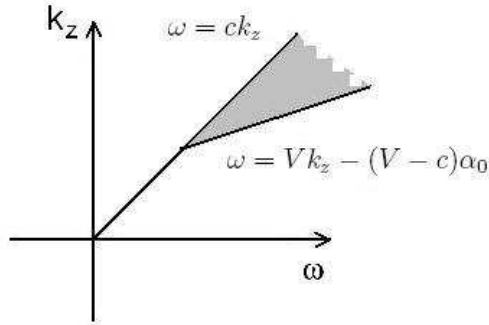


Figure 5: The spectrum (35), when written in terms of the spectral parameters ω and k_z , has its domain indicated by the shaded region.

and, by using identity 6.616 in Ref.[102], we get an expression[65] that can be directly integrated to furnish

$$\psi(\rho, \zeta, \eta) = \frac{X \exp \left\{ -\alpha_0 \left[(a - i\eta) - \frac{1}{\beta + 1} (s - i\zeta - X^{-1}) \right] \right\}}{(a - i\eta) - \frac{1}{\beta + 1} (s - i\zeta - X^{-1})}, \quad (37)$$

As far as we know, the new solution (37) is the first one to represent finite-energy NDWs completely free of backward components[65].

Totally forward, finite-energy superluminal NDW pulses. The finite-energy NDW (37) can be superluminal (peak-velocity $V > c$) or luminal (peak-velocity c) depending on the relative values of the constants a and s . To see this in a rigorous way, in connection with solution (37), in Ref.[65] it has been calculated how its global maximum of intensity (i.e, its peak), which is located on $\rho = 0$, develops in time. One then obtained the peak's motion by considering the field intensity of (37) on the z axis, i.e., $|\psi(0, \zeta, \eta)|^2$, at a given time t , and finding out the value of z at which the pulse presents a global maximum. It was called $z_p(t)$ (the peak's position) this value of z ; and the peak velocity evaluated as $dz_p(t)/dt$.

As shown in Ref.[65], superluminal finite-energy NDW pulses may be obtained from (37) by putting $a \gg s$. In this case, the spectrum $A(\alpha, \sigma)$ is well concentrated around the line $\alpha = \alpha_0$, and therefore in the plane (k_z, ω) this spectrum starts at $\omega_{\min} \approx c\alpha_0$ with an exponential decay, and the bandwidth $\Delta\omega \approx V/s$.

Defining the field depth Z as the distance over which the pulse's peak intensity remains

at least 25% of its initial value[†], one obtains[65] the depth of field

$$Z = \frac{\sqrt{3} a}{1 - \beta^{-1}},$$

which depends on a and $\beta = V/c$: Thus, the pulse can get large field depths by suitably adjusting the value of parameter a .

Figure 6 shows the space-time evolution, from the pulse's peak at $z_p = 0$ to $z_p = Z$, of a finite-energy superluminal NDW pulse represented by Eq.(37) with the following parameter values: $a = 20$ m, $s = 3.99 \times 10^{-6}$ m (note that $a \gg s$), $V = 1.005 c$ and $\alpha_0 = 1.26 \times 10^7 \text{ m}^{-1}$. For such a pulse, we have a frequency spectrum starting at $\omega_{\min} \approx 3.77 \times 10^{15} \text{ Hz}$ (with an exponential decay) and the bandwidth $\Delta\omega \approx 7.54 \times 10^{13} \text{ Hz}$. From these values and since $\Delta\omega/\omega_{\min} = 0.02$, it is a optical pulse with $\lambda_0 = 0.5 \mu\text{m}$ and time width of 13 fs. At the distance given by the field depth $Z = \sqrt{3} a/(1 - \beta^{-1}) = 6.96$ km the peak intensity is a fourth of its initial value. Moreover, it is interesting to note that, in spite of the intensity decrease, the pulse's spot size $\Delta\rho_0 = 7.5 \mu\text{m}$ remains constant during the propagation.

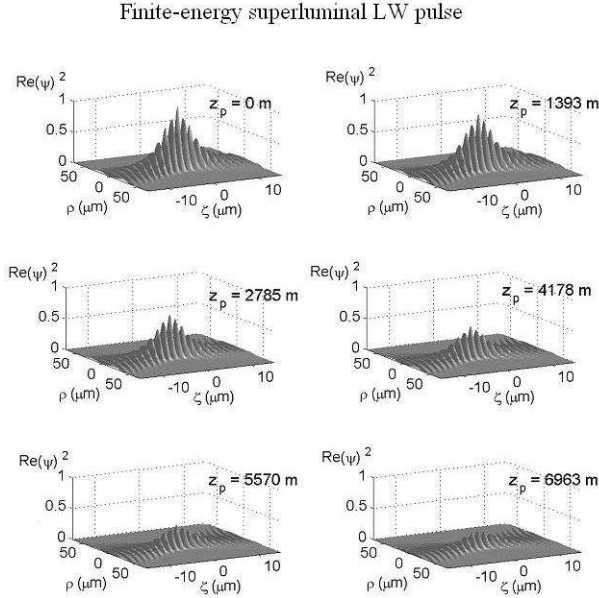


Figure 6: The space-time evolution, from the pulse's peak at $z_p = 0$ to $z_p = Z$, of a totally “forward”, finite-energy, superluminal NDW optical pulse represented by Eq.(37), with the following parameter values: $a = 20$ m, $s = 3.99 \times 10^{-6}$ m (note that $a \gg s$), $V = 1.005 c$ and $\alpha_0 = 1.26 \times 10^7 \text{ m}^{-1}$.

[†]We can expect that, while the pulse peak intensity is maintained, the same happens for its spatial form.

Totally “forward”, finite-energy luminal NDW pulses. Luminal finite energy NDW pulses can be obtained from Eq.(37) by making $s \gg a$ (more rigorously, for $s^2c \gg a^2V$). In this case, the spectrum $A(\alpha, \sigma)$ is well concentrated around the line $\sigma = 0$, and therefore in the plane (k_z, ω) it starts at $\omega_{\min} \approx c\alpha_0$ with an exponential decay and the bandwidth $\Delta\omega \approx c/a$.

On defining the field depth Z as the distance over which the pulse’s peak intensity remains at least 25% of its initial value, one obtains[65] the depth of field

$$Z = \frac{\sqrt{3}s}{\beta - 1} \quad (38)$$

which depends on s and $\beta = V/c$.

Here, we confine ourselves to depict in Figure 7 the space-time evolution of such a pulse, from $z_p = 0$ to $z_p = Z$. At the distance given by the field depth $Z = \sqrt{3}s/(\beta - 1) = 23.1$ km the peak intensity is just a fourth of its initial value.

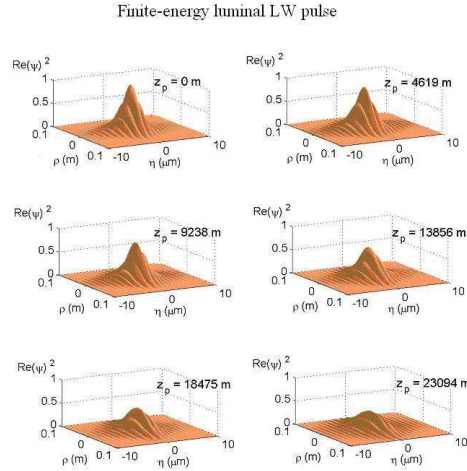


Figure 7: The space-time evolution, from the pulse’s peak at $z_p = 0$ to $z_p = Z$, of a totally “forward”, finite-energy, luminal NDW optical pulse represented by Eq.(37), with $a = 1.59 \times 10^{-6}$ m, $s = 1 \times 10^4$ m (note that $s \gg a$), $V = 1.5c$, $\alpha_0 = 1.26 \times 10^7$ m⁻¹.

We can see from the two examples above, and it can also be shown in a rigorous way, that the superluminal NDW pulses obtained from solution (37) are superior than the luminal ones obtained from the same solution, in the sense that the former can possess large field depths and, at the same time, be endowed with strong transverse field concentrations. To obtain more interesting and efficient luminal NDW pulses we should use[12, 65] spectra concentrated around the line $\sigma = \sigma_0 > 0$.

3.1 A general functional expression for whatever totally-forward NDW pulses

In the literature concerning the NDWs[64] some interesting approaches appear, yielding functional expressions which describe NDWs in closed form. Although interesting, even the NDWs obtained from those approaches possess backward components in their spectral structure.

A general functional expression, capable of furnishing whatever totally-forward NDW pulses, is, however[65]:

$$\psi(\rho, \phi, \zeta, \eta) = e^{i\nu\phi} \left(\frac{\gamma^{-1}\rho}{s - i\zeta + X^{-1}} \right)^\nu X F(S) , \quad (39)$$

with $F(\cdot)$ an arbitrary function, and X the ordinary X-wave (31), while S is

$$S = -i\eta - \frac{1}{\beta + 1}(s - i\zeta - X^{-1}) .$$

Equation (39) is indeed an exact solution to the wave equation that can yield both ideal and finite-energy NDW pulses, with superluminal or luminal peak velocities. And the NDW solutions obtained from Eq.(39) are totally free of backward components under the only condition that the chosen function $F(S)$ be regular and free of singularities at all space-time points (ρ, ϕ, z, t) .

4 Method for the *Analytic* Description of *Truncated* Beams

If we are allowed to set forth some more formal material, we like to present now an *analytic* method for describing important beams, *truncated* by finite apertures, in the Fresnel regime. The method works in Electromagnetism (Optics, Microwaves,...), as well as in Acoustics, etcetera. But we shall here confine ourselves to Optics, for conciseness' sake.

Our method[77], rigorous and effective but rather simple, is based on appropriate superpositions of Bessel-Gauss beams, and in the Fresnel regime is able to describe in analytic form the 3D evolution of important waves, like Bessel beams, plane waves, gaussian beams and Bessel-Gauss beams, when truncated by finite apertures. One of the advantages of our mathematical method is that one can get in few seconds, or minutes, high-precision results which normally require quite long times of numerical simulation. Indeed, also the coefficients of the Bessel-Gauss beam superpositions result to be obtainable in a direct way, without any need of numerical evaluations or optimizations.

4.1 The Method

We shall leave understood in all solutions the harmonic time-dependence term $\exp(-i\omega t)$. In the *paraxial approximation*, an axially symmetric monochromatic wave field can be evaluated, knowing its shape on the $z = 0$ plane, through the Fresnel diffraction integral in cylindrical coordinates:

$$\Psi(\rho, z) = \frac{-ik}{z} e^{i(kz + \frac{k\rho^2}{2z})} \int_0^\infty \Psi(\rho', 0) e^{ik\frac{\rho'^2}{2z}} J_0\left(k\frac{\rho\rho'}{z}\right) \rho' d\rho', \quad (40)$$

where, as usual, $k = 2\pi/\lambda$ is the wavenumber, and λ the wavelength. In this equation, ρ' reminds us that the integration is being performed on the plane $z = 0$; thus, $\Psi(\rho', 0)$ does simply indicate the field value on $z = 0$. An important solution is obtained by considering on the $z = 0$ plane the ‘‘excitation’’ given by

$$\Psi(\rho', 0) = \Psi_{BG}(\rho', 0) = AJ_0(k_\rho \rho') \exp(-q\rho'^2), \quad (41)$$

which[103] produces the so-called Bessel-Gauss beam[104]:

$$\Psi_{BG}(\rho, z) = -\frac{ikA}{2zQ} e^{ik(z + \frac{\rho^2}{2z})} J_0\left(\frac{ik k_\rho \rho}{2zQ}\right) e^{-\frac{1}{4Q}(k_\rho^2 + \frac{k^2 \rho^2}{z^2})}, \quad (42)$$

which is a Bessel beam transversally modulated by the Gaussian function. Quantity $Q = q - ik/2z$, and k_ρ is a constant (namely, the transverse wavenumber associated with the modulated Bessel beam). When $q = 0$, the Bessel-Gauss beam results in the well-known Gaussian beam. The Gaussian beam, and Bessel-Gauss', Eq.(42), are among the few solutions to the Fresnel diffraction integral that can be obtained analytically. The situation gets much more complicated, however, when facing beams truncated in space by finite circular apertures: For instance, a Gaussian beam, or a Bessel beam, or a Bessel-Gauss beam, truncated via an aperture with radius R . In this case, the upper limit of the integral in Eq.(40) becomes the aperture radius, and the analytic integration becomes very difficult, requiring recourse to lengthy numerical calculations.

Let us now go on to our method for the description of truncated beams, characterized by simplicity and, in most cases, total analyticity. Let us start with the Bessel-Gauss beam, Eq.(42), and consider the solution given by the following superposition of such beams:

$$\Psi(\rho, z) = -\frac{ik}{2z} e^{ik(z + \frac{\rho^2}{2z})} \sum_{n=-N}^N \frac{A_n}{Q_n} J_0\left(\frac{ik k_\rho \rho}{2zQ_n}\right) e^{-\frac{1}{4Q_n}(k_\rho^2 + \frac{k^2 \rho^2}{z^2})}, \quad (43)$$

quantities A_n being constants, and Q_n given by

$$Q_n = q_n - \frac{ik}{2z}, \quad (44)$$

where the q_n are constants that can assume *complex values*. Notice that in this superposition all beams possess the same value of k_ρ . We want the solution (43) to be able

to represent beams truncated by circular apertures, in the case, as we know, of Bessel beams, gaussian beams, Bessel-Gauss beams, and plane waves.

Given one of such beams, truncated at $z = 0$ by an aperture with radius R , we have to determine the coefficients A_n and q_n in such a way that Eq.(43) represents with fidelity the resulting beam: If the truncated beam on the $z = 0$ plane is given by $V(\rho)$, we have to obtain $\Psi(\rho, 0) = V(\rho)$; that is to say

$$V(\rho) = J_0(k_\rho \rho) \sum_{n=-N}^N A_n e^{-q_n \rho^2} . \quad (45)$$

The r.h.s. of this equation is indeed nothing but a superposition of Bessel-Gauss beams, all with the same value of k_ρ , at $z = 0$ [namely, each one of such beams is written at $z = 0$ according to Eq.(41)].

One has to get the values of the A_n and q_n , as well as of N , from Eq.(45). Once these values have been obtained, the field emanated by the finite circular aperture located at $z = 0$ will be given by Eq.(43). Remembering that the q_n can be complex, let us make the following choices:

$$q_n = q_R + iq_{In} , \quad \text{with} \quad q_{In} = -\frac{2\pi}{L} n , \quad (46)$$

where $q_R > 0$ is the real part of q_n , having the *same value* for every n ; q_{In} is the imaginary part of q_n ; and L is a constant with the dimensions of a square length.

With such choices, and assuming $N \rightarrow \infty$, Eq.(45) gets written as

$$V(\rho) = J_0(k_\rho \rho) \exp(-q_R \rho^2) \sum_{n=-\infty}^{\infty} A_n \exp\left(i\frac{2\pi n}{L} \rho^2\right) , \quad (47)$$

which has then to be exploited for obtaining the values of A_n , k_ρ , q_R and L .

In the cases of a truncated Bessel beam (TB) or of a truncated Bessel-Gauss beam (TBG), it is natural to choose quantity k_ρ in Eq.(47) equal to the corresponding beam transverse wavenumber. In the case of a truncated Gaussian beam (TG) or of a truncated plane wave (TP), by contrast, in Eq.(47) it is natural to choose $k_\rho = 0$. In all cases, the product

$$\exp(-q_R \rho^2) \sum_{n=-\infty}^{\infty} A_n \exp\left(i\frac{2\pi n}{L} \rho^2\right) , \quad (48)$$

in Eq.(47) has to represent:

- (i) a function $\text{circ}(\rho/R)$, in the TB or TP cases;
- (ii) a function $\exp(-q \rho^2) \text{circ}(\rho/R)$, that is, a circ function multiplied by a Gaussian function, in the TBG or TG cases. Of course (i) is a particular case of (ii) with $q = 0$. It may be useful to recall that the circ-function is the step-function in the cylindrically symmetric case. Quantity R is still the aperture radius, and $\text{circ}(\rho/R) = 1$ when $0 \leq \rho \leq R$, and equals 0 elsewhere.

Let us now show how expression (48) can approximately represent the above functions, given in (i) and (ii). To such an aim, let us consider a function $G(r)$ defined on an interval $|r| \leq L/2$ and endowed with the Fourier expansion

$$G(r) = \sum_{n=-\infty}^{\infty} A_n \exp(i2\pi nr/L) \quad \text{for } |r| \leq L/2, \quad (49)$$

where r and L , having the dimensions of a square length, are expressed in square meters (m^2). Suppose now the function $G(r)$ to be given by

$$G(r) = \begin{cases} \exp(q_R r) \exp(-q r) & \text{for } |r| \leq R^2 \\ 0 & \text{for } R^2 < |r| < L/2, \end{cases} \quad (50)$$

where q is a given constant. Then, the coefficients A_n in the Fourier expansion of $G(r)$ will be given by:

$$A_n = \frac{1}{L(q_R - q) - i2\pi n} \left(e^{(q_R - q - i\frac{2\pi}{L}n)R^2} - e^{-(q_R - q - i\frac{2\pi}{L}n)R^2} \right). \quad (51)$$

Writing now

$$r = \rho^2, \quad (52)$$

we get that quantity (48) in Eqs.(49,50) can be written as

$$e^{-q_R \rho^2} \sum_{n=-\infty}^{\infty} A_n e^{i2\pi n \rho^2 / L} = \begin{cases} e^{-q \rho^2} & \text{for } 0 \leq \rho \leq R \\ 0 & \text{for } R < \rho \leq \sqrt{L/2} \\ e^{-q_R \rho^2} f(\rho) \approx 0 & \text{for } \rho > \sqrt{L/2}, \end{cases} \quad (53)$$

where the coefficients A_n are still given by Eq.(51), and $f(\rho)$ is a function existing on shorter and shorter space intervals, assuming as its maximum value $\exp[(q_R - q)R^2]$, when $q_R > q$, or 1, when $q_R \leq q$. Since $\sqrt{L/2} > R$, for suitable choices of q_R and L , we shall have that $\exp(-q_R \rho^2) f(\rho) \approx 0$ for $\rho \geq \sqrt{L/2}$.

Therefore, we obtain that

$$e^{-q_R \rho^2} \sum_{n=-\infty}^{\infty} A_n e^{i2\pi n \rho^2 / L} \approx e^{-q \rho^2} \text{circ}(\rho/R), \quad (54)$$

which corresponds to case (i), when $q = 0$, and to case (ii). Let us recall once more that the A_n are given by Eqs.(51).

On the basis of what was shown before, we have now in our hands a rather efficient method for describing important beams, truncated by finite apertures: Namely, the TB

(truncated Bessel), TG (truncated Gauss), TBG (truncated Besse-Gauss), and TP (truncated Plane wave) beams. Indeed, it is enough to choose the desired field, truncated by a circular aperture with radius R , and describe it at $z = 0$ by our Eq.(47).

Precisely:

- In the TBG case: the value of k_ρ in Eq.(47) is the transverse wavenumber of the Bessel beam modulated by the Gaussian function; A_n is given in Eq.(51); q is related to the Gaussian function width at $z = 0$. The values L and q_R , and the number N of terms in the series (47), are chosen so as to guarantee a faithful description of the beam at $z = 0$ when truncated by a circular aperture with radius R .
- The TB, TG and TP are special cases of TBG: in TB, $q = 0$; in TG, $k_\rho = 0$; and in TP, $k_\rho = 0$ and $q = 0$

In conclusion, *once we know the chosen beam on the truncation plane ($z = 0$), the beam emanated by the finite aperture will then be given by solution (43)*. Further details can be found in [77].

Let us go on to an important example.

4.2 Application of the method to a truncated Bessel beam

For the sake of brevity, we apply our method only to the analytic description of the truncated Bessel beam.

Let us consider a Bessel beam, with wavelength of 632.8 nm, truncated at $z = 0$ by a circular aperture with radius R ; that is to say, let us start from $\Psi_{TB}(\rho, 0) = J_0(k_\rho \rho) \text{circ}(\rho/R)$. Let us choose $R = 3.5$ mm, and the transverse wavenumber $k_\rho = 4.07 \cdot 10^4 \text{ m}^{-1}$, which corresponds to a beam spot with radius approximatively equal to $\Delta\rho = 59 \mu\text{m}$.

At $z = 0$ the field is described by Eq.(47), where the A_n are given by Eq.(51) and where $q = 0$. In this case, a quite good result can be obtained by the choice $L = 3R^2$, $q_R = 6/L$ and $N = 23$. Let us stress that, since such a choice is not unique, very many alternative sets of values L and q_R exist, which yield excellent results as well.

In the figures (8), image (a) depicts the field given by Eq.(47): it represents with high fidelity the Bessel beam truncated at $z = 0$. The resulting field, emanated by the aperture, is given by solution (43), and its intensity is shown in image (b). One can see that the result really corresponds to a Bessel beam truncated by a finite aperture.

5 Subluminal Non-diffracting Waves (or Bullets)

Let us now obtain in a simple way Non-diffracting *subluminal* Pulses, always as exact analytic solutions to the wave equations.[19] We shall adopt in this Section a less formal language (perhaps more intuitive, or more physical), and we shall confine to ideal

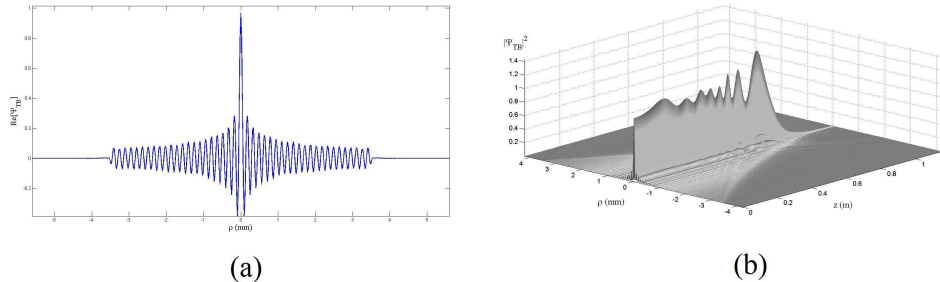


Figure 8: (Color online)(a) Field given by Eq.(47), representing a Bessel beam at $z = 0$, with $k_\rho = 4.07 \cdot 10^4 \text{ m}^{-1}$ and truncated by a finite circular aperture with radius $R = 3.5 \text{ mm}$. The coefficients A_n are given by Eq.(51), with $q = 0$, $L = 3R^2$, $q_R = 6/L$ and $N = 23$. (b) Intensity of a Bessel beam truncated by a finite aperture, as given by solution (43).

solutions, but such solutions will be constructed for arbitrarily chosen frequencies and bandwidths, and once more avoiding any recourse to the non-causal (backward moving) components. Also the new solutions can be suitable superpositions of —zeroth-order, in general— Bessel beams, which can be performed by integrating either w.r.t. the angular frequency ω , or w.r.t. the longitudinal wavenumber k_z : Both approaches are treated below. The first one is powerful enough; we sketch the second approach as well, however, since it allows also dealing —from a new starting point— with the limiting case of *zero-speed* solutions: Namely, it furnishes a new way, in terms of *continuous* spectra, for obtaining such (“frozen”) waves[4, 5, 6, 7] so promising also from the point of view of the applications. Some attention is successively paid to the known role of Special Relativity, and to the fact that the NDWs are expected to be transformed one into the other by suitable Lorentz Transformations. We are moreover going to mention the case of non axially-symmetric solutions, in terms of higher order Bessel beams. We keep fixing our attention especially on electromagnetism and optics: But let us repeat that results of the same kind are valid whenever an essential role is played by a wave-equation [like in acoustics, seismology, geophysics, elementary particle physics (as we shall explicitly see in the slightly different case of the Schroedinger equation), and also gravitation (for which we have recently got stimulating new results), and so on].

Subluminal NDWs can be obtained too by suitable superpositions of Bessel beams,[19], as in the other cases, but have been rather neglected for the mathematical difficulties in getting analytic expressions for them, since the superposition integral runs over a finite interval. Therefore, almost all the few papers devoted to the subluminal NDWs had recourse to the paraxial[96] approximation[100], or to numerical simulations[105]. Only *one* analytic solution was known[31, 32, 33, 58, 65], biased by the inconvenience that its frequency spectrum is very large, that it does not possess a well-defined central

frequency, and that backward-travelling[56, 54] components were needed for constructing it. In this Section we construct, on the contrary, non-diffracting exact solutions with any spectra, in any frequency bands and for any bandwidths; and without employing[12, 52] backward-traveling components. One can arrive at such (analytic) solutions, both in the case of integration over the Bessel beams' angular frequency ω , and of integration over their longitudinal wavenumber k_z .

5.1 A first method for constructing physically acceptable, subluminal Non-diffracting Pulses

Axially-symmetric solutions to the scalar wave equation are known to be superpositions of zero-order Bessel beams over the angular frequency ω and the longitudinal wavenumber k_z : That is, in cylindrical co-ordinates,

$$\Psi(\rho, z, t) = \int_0^\infty d\omega \int_{-\omega/c}^{\omega/c} dk_z \bar{S}(\omega, k_z) J_0 \left(\rho \sqrt{\frac{\omega^2}{c^2} - k_z^2} \right) e^{ik_z z} e^{-i\omega t}, \quad (55)$$

where, as usual, $k_\rho^2 \equiv \omega^2/c^2 - k_z^2$ is the transverse wavenumber; and quantity k_ρ^2 has to be positive since evanescent waves are here excluded. We already know that the condition characterizing a non-diffracting wave is the existence[54, 106] of a linear relation between longitudinal wavenumber k_z and frequency ω for all the Bessel beams entering the superposition; that is to say, in the chosen spectrum for each Bessel beam it has to be[12, 50]

$$\omega = v k_z + b \quad (56)$$

with $b \geq 0$. [More generally, as shown in Ref.[12], in the plane ω, k_z the chosen spectrum has to call into the play, if not exactly such a line, at least a region in the proximity of a straight-line of that type. In the latter case one obtains solutions endowed with finite energy, and therefore a finite "depth of field"].

The requirement (56) is a specific space-time coupling, implied by the chosen spectrum \bar{S} . Let us recall that Eq.(56) has to be obeyed by the spectra of any one of the three possible types (subluminal, luminal or Superluminal) of non-diffracting pulses: Indeed, with the choice (56), the pulse re-gains its initial shape after the space-interval $\Delta z_1 = 2\pi v/b$. [But the more general case can be also considered[12, 53] when b assumes any values $b_m = m b$ (with m an integer), and the periodicity space-interval becomes $\Delta z_m = \Delta z_1/m$. We are referring ourselves, now, to the real (or imaginary) part of the pulse, since its magnitude is endowed with rigid motion].

Let us first derive in the subluminal case the only exact solution known till recent time, the Mackinnon's[31] one, represented by Eq.(63) below. Since the transverse wavenumber k_ρ of each Bessel beam entering Eq.(55) has to be real, it can be easily shown (as first noticed in [105]) that in the subluminal case b cannot vanish, but it must be $b > 0$. Then,

on using conditions (56) and $b > 0$, the subluminal localized pulses can be expressed as integrals over the frequency only:

$$\Psi(\rho, z, t) = \exp\left[-ib\frac{z}{v}\right] \int_{\omega_-}^{\omega_+} d\omega S(\omega) J_0(\rho k_\rho) \exp\left[i\omega\frac{\zeta}{v}\right], \quad (57)$$

where now

$$k_\rho = \frac{1}{v} \sqrt{2b\omega - b^2 - (1 - v^2/c^2)\omega^2} \quad (58)$$

with

$$\zeta \equiv z - vt \quad (59)$$

and with

$$\begin{cases} \omega_- = \frac{b}{1 + v/c} \\ \omega_+ = \frac{b}{1 - v/c} \end{cases}. \quad (60)$$

As anticipated, the Bessel beam superposition in the subluminal case is an integration over a finite interval of ω , which also does show that the backward-travelling components correspond to the interval $\omega_- < \omega < b$. [It could be noticed that Eq.(57) does not represent the most general exact solution, which on the contrary is a *sum*[53] of such solutions for the various possible values of b mentioned above: That is, for the values $b_m = mb$ with spatial periodicity $\Delta z_m = \Delta z_1/m$. But we can confine ourselves to solution (57) without any real loss of generality, since the actual problem is evaluating in analytic form the integral entering Eq.(57). For any mathematical and physical details, see Ref.[53]].

Now, if one adopts the change of variable

$$\omega \equiv \frac{b}{1 - v^2/c^2} \left(1 + \frac{v}{c}s\right) \quad (61)$$

equation (57) becomes[105]

$$\begin{aligned} \Psi(\rho, z, t) &= \frac{b}{c} \frac{v}{1 - v^2/c^2} \exp\left[-i\frac{b}{v}z\right] \exp\left[i\frac{b}{v} \frac{1}{1 - v^2/c^2} \zeta\right] \\ &\times \int_{-1}^1 ds S(s) J_0\left(\frac{b}{c} \frac{\rho}{\sqrt{1 - v^2/c^2}} \sqrt{1 - s^2}\right) \exp\left[i\frac{b}{c} \frac{1}{1 - v^2/c^2} \zeta s\right]. \end{aligned} \quad (62)$$

In the following we shall adhere —as it is an old habit of ours— to some symbols standard in Special Relativity, since the whole topic of subluminal, luminal and Superluminal NDWs is strictly connected[13, 14, 94] with the principles and structure of SR [cf.[92, 110] and refs. therein], as we shall mention also in the specific remarks which follow below). Namely, we put $\beta \equiv v/c$ and $\gamma \equiv 1/\sqrt{1 - \beta^2}$.

Equation (62) has till now yielded *one* analytic solution, for $S(s) = \text{constant}$: the *Mackinnon solution*[31, 58, 33, 78]

$$\begin{aligned} \Psi(\rho, \zeta, \eta) &= 2\frac{b}{c}v\gamma^2 \exp\left[i\frac{b}{c}\beta\gamma^2\eta\right] \\ &\times \text{sinc}\sqrt{\frac{b^2}{c^2}\gamma^2(\rho^2 + \gamma^2\zeta^2)}, \end{aligned} \quad (63)$$

which however, for its above-mentioned drawbacks, is endowed with little physical and practical interest. In Eq.(63) the sinc function has the ordinary definition $\text{sinc } x \equiv (\sin x)/x$, and

$$\eta \equiv z - Vt, \quad \text{with } V \equiv \frac{c^2}{v}, \quad (64)$$

where V and v are related by the *de Broglie relation*. Notice that Ψ in Eq.(63), and in the following ones, is eventually a function (besides of ρ) of z, t only via quantities ζ and η .

However, we can construct further subluminal pulses, corresponding to whatever spectrum and devoid of backward-moving components, just by exploiting the fact that in our equation (62) the integration interval is finite: That it, by transforming it into a good, instead of a harm. Let us first observe that Eq.(62) will also yield exact, analytic solutions for *any* exponential spectra of the type

$$S(\omega) = \exp\left[\frac{i2n\pi\omega}{\Omega}\right], \quad (65)$$

with n any integer number: Which means for any spectra of this type it holds $S(s) = \exp[in\pi/\beta] \exp[in\pi s]$, as can be easily checked. In Eq.(65) we have set $\Omega \equiv \omega_+ - \omega_-$. In this more general case, the solution writes

$$\begin{aligned} \Psi(\rho, \zeta, \eta) &= 2b\beta\gamma^2 \exp\left[i\frac{b}{c}\beta\gamma^2\eta\right] \\ &\times \exp\left[in\frac{\pi}{\beta}\right] \text{sinc}\sqrt{\frac{b^2}{c^2}\gamma^2\rho^2 + \left(\frac{b}{c}\gamma^2\zeta + n\pi\right)^2}. \end{aligned} \quad (66)$$

Notice that also in Eq.(66) quantity η is defined as in Eqs.(64) above, where V and v obey the de Broglie relation $vV = c^2$, the subluminal quantity v being the velocity of the pulse envelope, and V playing the role (in the envelope's interior) of a superluminal phase velocity.

We now take *advantage* of the finiteness of the integration limits for expanding any arbitrary spectra $S(\omega)$ in a Fourier series in the interval $\omega_- \leq \omega \leq \omega_+$; that is:

$$S(\omega) = \sum_{n=-\infty}^{\infty} A_n \exp\left[+in\frac{2\pi}{\Omega}\omega\right], \quad (67)$$

where (we went back, now, from the s to the ω variable):

$$A_n = \frac{1}{\Omega} \int_{\omega_-}^{\omega_+} d\omega S(\omega) \exp \left[-in \frac{2\pi}{\Omega} \omega \right] \quad (68)$$

quantity Ω being defined above.

Then, on remembering the special, ‘‘Mackinnon-type’’ solution (66), we can infer from expansion (65) that, for any arbitrary spectral function $S(\omega)$, one can work out a rather general axially-symmetric analytic solution for the subluminal case:

$$\begin{aligned} \Psi(\rho, \zeta, \eta) = & 2b\beta\gamma^2 \exp \left[i \frac{b}{c} \beta \gamma^2 \eta \right] \\ & \times \sum_{n=-\infty}^{\infty} A_n \exp \left[in \frac{\pi}{\beta} \right] \operatorname{sinc} \sqrt{\frac{b^2}{c^2} \gamma^2 \rho^2 + \left(\frac{b}{c} \gamma^2 \zeta + n\pi \right)^2}, \end{aligned} \quad (69)$$

coefficients A_n being still given by Eq.(68).

The present approach presents several advantages. We can easily choose spectra localized within the prefixed frequency interval (optical waves, microwaves, etc.) and endowed with the desired bandwidth. Moreover, we have seen that spectra can now be chosen such that they have zero value in the region $\omega_- \leq \omega \leq b$, which is responsible for the backward-traveling components of the subluminal pulse. Even when the adopted spectrum $S(\omega)$ does not possess a known Fourier series (so that the coefficients A_n cannot be exactly evaluated via Eq.(68), one can calculate approximately such coefficients without meeting any problem, since our general solutions (69) will still be exact solutions.

Let us set forth some examples.

5.2 Examples

In general, optical pulses generated in the lab possess a spectrum centered at some frequency value, ω_0 , called the carrier frequency. The pulses can be, for instance, ultra-short, when $\Delta\omega/\omega_0 \geq 1$; or quasi-monochromatic, when $\Delta\omega/\omega_0 \ll 1$, where $\Delta\omega$ is the spectrum bandwidth.

These kinds of spectra can be mathematically represented by a gaussian function, or by functions with similar behaviour. One can find various examples In Refs.[11, 19].

First example — Let us consider, e.g., a gaussian spectrum:

$$S(\omega) = \frac{a}{\sqrt{\pi}} \exp \left[-a^2(\omega - \omega_0)^2 \right] \quad (70)$$

whose values are negligible outside the frequency interval $\omega_- < \omega < \omega_+$ over which the Bessel beams superposition in Eq.(57) is made, it being $\omega_- = b/(1+\beta)$ and $\omega_+ = b/(1-\beta)$. [Let us stress that, once v and b have been fixed, the values of a and ω_0 can afterwards

be selected in order to kill the backward-travelling components, that correspond, as we know, to $\omega < b$]. The Fourier expansion in Eq.(67), which yields, with the above spectral function (70), the coefficients

$$A_n \simeq \frac{1}{W} \exp \left[-in \frac{2\pi}{\Omega} \omega_0 \right] \exp \left[\frac{-n^2 \pi^2}{a^2 W^2} \right], \quad (71)$$

constitutes an excellent representation of the gaussian spectrum (70) in the interval $\omega_- < \omega < \omega_+$ (provided that, as we requested, our gaussian spectrum does get *negligible* values outside the frequency interval $\omega_- < \omega < \omega_+$). In other words, a subluminal pulse with frequency spectrum (70) can be written as Eq.(69), with the coefficients A_n given by Eq.(71): the evaluation of such coefficients A_n being rather simple. Let us repeat that, even if the values of the A_n are obtained via a (rather good, by the way) approximation, we based ourselves on the *exact* solution Eq.(69).

One can, for instance, obtain exact solutions representing subluminal pulses for optical frequencies: Cf. Figs.9. The construction of the considered pulse results already satisfactory when considering about 51 terms ($-25 \leq n \leq 25$) in the series entering Eq.(69).

Figures 9 show that pulse, evaluated just by summing the mentioned fifty-one terms: Fig.(a) depicts the orthogonal projection of the pulse intensity; Fig.(b) shows the three-dimensional intensity pattern of the *real part* of the pulse, which reveals the carrier wave oscillations.

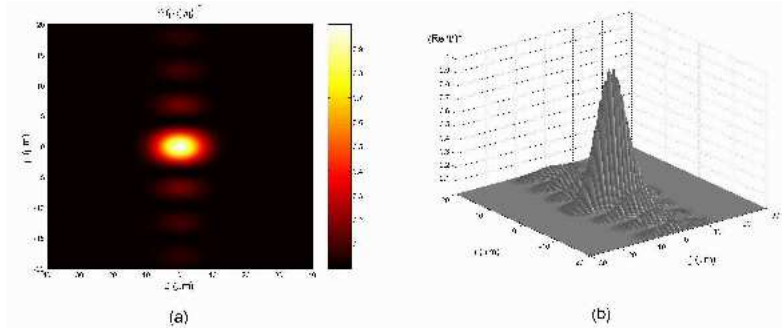


Figure 9: **(a)** The intensity orthogonal projection for a pulse corresponding to Eqs.(70,71) in the case of an optical frequency: Namely, for a subluminal pulse with velocity $v = 0.99 c$, carrier angular frequency $\omega_0 = 2.4 \times 10^{15}$ Hz (that is, $\lambda_0 = 0.785 \mu\text{m}$) and bandwidth (FWHM) $\Delta\omega = \omega_0/20 = 1.2 \times 10^{14}$ Hz; which results to be an optical pulse of 24 fs. One has also to specify a value for the the frequency: let it be $b = 3 \times 10^{13}$ Hz; as a consequence one has $\omega_- = 1.507 \times 10^{13}$ Hz and $\omega_+ = 3 \times 10^{15}$ Hz. [This is exactly a case in which the pulse has no backward-traveling components, since the chosen spectrum possesses totally negligible values for $\omega < b$]; **(b)** The three-dimensional intensity pattern of the *real part* of the same pulse, which reveals the carrier wave oscillations.

Let us stress (see below) that the ball-like shape for the field intensity is typically associated with the subluminal NDWs, while the typical Superluminal ones are known to be X-shaped[9, 14, 94], as predicted since long by special relativity in its “non-restricted” version: See Refs.[92, 110, 14, 13, 37] and refs therein. It can be indeed noted that each term of the series in Eq.(69) corresponds to an ellipsoid or, more specifically, to a spheroid, for each velocity v .

A second example — Let us consider now the very simple case when, within the integration limits ω_-, ω_+ , the complex exponential spectrum (65) is replaced by the real function (still linear in ω)

$$S(\omega) = \frac{a}{1 - \exp[-a(\omega_+ - \omega_-)]} \exp[a(\omega - \omega_+)] , \quad (72)$$

with a a positive number [for $a = 0$ one goes back to the Mackinnon case]. Spectrum (72) is exponentially concentrated in the proximity of ω_+ , where it reaches its maximum value, and (on the left of ω_+) becomes more and more concentrated as the arbitrarily chosen value of a increases; its frequency bandwidth being $\Delta\omega = 1/a$.

On performing the integration as in the case of spectrum (65), instead of solution (66) in the present case one eventually gets the solution

$$\begin{aligned} \Psi(\rho, \zeta, \eta) = & \frac{2ab\beta\gamma^2 \exp[ab\gamma^2] \exp[-a\omega_+]}{1 - \exp[-a(\omega_+ - \omega_-)]} \\ & \times \exp\left[i\frac{b}{c}\beta\gamma^2\eta\right] \operatorname{sinc}\left[\frac{b}{c}\gamma^2\sqrt{\gamma^{-2}\rho^2 - (av + i\zeta)^2}\right] . \end{aligned} \quad (73)$$

This Eq.(73) appears to be the simplest closed-form solution, after Mackinnon’s, since both of them do not need any recourse to series expansions. In a sense, our solution (73) may be regarded as the subluminal analogue of the (Superluminal) X-wave solution; a difference being that the standard X-shaped solution has a spectrum starting with 0, where it assumes its maximum value, while in the present case the spectrum starts at ω_- and gets increasing afterwards, till ω_+ . More important is to observe that the gaussian spectrum has a priori two advantages w.r.t. Eq.(72): It may be more easily centered around any value ω_0 of ω , and, when increasing its concentration in the surroundings of ω_0 , the spot transverse width does not increase indefinitely, but tends to the spot-width of a Bessel beam with $\omega = \omega_0$ and $k_z = (\omega_0 - b)/V$, at variance with what happens for spectrum (72). Anyway, solution (73) is noticeable, since it is really *the simplest* one. An example is consituted by Figure 37 in [11], referring to an optical pulse of 0.2 ps.

5.3 A second method for constructing subluminal Non-diffracting Pulses

The previous method appears to be very efficient for finding out analytic subluminal NDWs, but it loses its validity in the limiting case $v \rightarrow 0$, since for $v = 0$ it is $\omega_- \equiv \omega_+$

and the integral in Eq.(57) degenerates, furnishing a null value. By contrast, we are interested also in the $v = 0$ case, since it corresponds, as we said, to some of the most interesting, and potentially useful, NDWs: That is, to the “stationary” solutions to the wave equations endowed with a *static* envelope, and that we call Frozen Waves. Before going on, let us recall that the theory of Frozen Waves was initially developed in Refs.[6, 4], by having recourse to discrete superpositions in such a way to bypass the need of numerical simulations. [In the case of continuous superpositions, some numerical simulations had been performed in Refs.[107]]. However, the method presented in this subsection does allow finding out analytic exact solutions, without any need of numerical simulations, also for Frozen Waves consisting in *continuous superpositions*.

Actually, we are going to see that the present method works regardless of the chosen field-intensity shape, and in regions with size of the order of the wavelength. It is possible to get such results by starting again from Eq.(55), with constraint (56), but going on — this time— to integrals over k_z , instead of over ω . It is enough to write relation (56) in the form $k_z = (\omega - b)/v$, for expressing the exact solutions (55) as

$$\Psi(\rho, z, t) = \exp[-ibt] \int_{k_z \min}^{k_z \max} dk_z S(k_z) J_0(\rho k_\rho) \exp[i\zeta k_z], \quad (74)$$

with

$$k_z \min = \frac{-b}{c} \frac{1}{1 + \beta}; \quad k_z \max = \frac{b}{c} \frac{1}{1 - \beta} \quad (75)$$

and with

$$k_\rho^2 = -\frac{k_z^2}{\gamma^2} + 2\frac{b}{c}\beta k_z + \frac{b^2}{c^2}, \quad (76)$$

where quantity ζ is still defined according to Eq.(59), always with $v < c$.

One can show that the unique exact solution previously known[31] may be rewritten in form (75) *with* $S(k_z) = \text{constant}$. Then, on following the same procedure exploited in our first method, one can again observe [11] that any spectra $S(k_z)$ can be expanded, on the interval $k_z \min < k_z < k_z \max$, into the Fourier series:

$$S(k_z) = \sum_{n=-\infty}^{\infty} A_n \exp\left[+in\frac{2\pi}{K}k_z\right], \quad (77)$$

with coefficients given now by

$$A_n = \frac{1}{K} \int_{k_z \min}^{k_z \max} dk_z S(k_z) \exp\left[-in\frac{2\pi}{K}k_z\right] \quad (78)$$

where $K \equiv k_z \max - k_z \min$.

At the end of the whole procedure[11], the general exact solution representing a subluminal NDW, for any spectra $S(k_z)$, can be eventually written

$$\Psi(\rho, \zeta, \eta) = 2\frac{b}{c}\gamma^2 \exp\left[i\frac{b}{c}\beta\gamma^2\eta\right]$$

$$\times \sum_{n=-\infty}^{\infty} A_n \exp[in\pi\beta] \operatorname{sinc} \sqrt{\frac{b^2}{c^2} \gamma^2 \rho^2 + \left(\frac{b}{c} \gamma^2 \zeta + n\pi\right)^2}, \quad (79)$$

whose coefficients are expressed in Eq.(78), and where quantity η is defined as above, in Eq.(64).

Interesting examples could be easily worked out.

6 “Stationary” solutions with zero-speed envelopes: *Frozen Waves*

Here, we shall refer ourselves to the (second) method, expounded above. Our solution (79), for the case of envelopes *at rest*, that is, in the case $v = 0$ [which implies $\zeta = z$], becomes

$$\Psi(\rho, z, t) = 2 \frac{b}{c} \exp[-ibt] \sum_{n=-\infty}^{\infty} A_n \operatorname{sinc} \sqrt{\frac{b^2}{c^2} \rho^2 + \left(\frac{b}{c} z + n\pi\right)^2}, \quad (85)$$

with coefficients A_n given by Eq.(78) with $v = 0$, so that its integration limits simplify into $-b/c$ and b/c , respectively. Thus, one gets

$$A_n = \frac{c}{2b} \int_{-b/c}^{b/c} dk_z S(k_z) \exp[-in \frac{c\pi}{b} k_z]. \quad (83')$$

Equation (85) is a new exact solution, corresponding to “stationary” beams with a *static* intensity envelope. Let us observe, however, that even in this case one has energy propagation, as it can be easily verified from the power flux $\mathbf{S}_s = -\nabla \Psi_{\mathcal{R}} \partial \Psi_{\mathcal{R}} / \partial t$ (scalar case) or from the Poynting vector $\mathbf{S}_v = (\mathbf{E} \wedge \mathbf{H})$ (vectorial case: the condition being that $\Psi_{\mathcal{R}}$ be a single component, A_z , of the vector potential \mathbf{A}).[14] We have indicated by $\Psi_{\mathcal{R}}$ the real part of Ψ . For $v = 0$, Eq.(56) becomes $\omega = b \equiv \omega_0$, so that the particular subluminal waves endowed with null velocity are actually monochromatic beams. [Let us explicitly observe that for smaller and smaller speeds the subluminal NDWs become *pulses* more and more localized in space: However, for $v = 0$ the frequency bandwidth becomes zero, and we end up no longer with pulses but with *beams*].

We seize the present opportunity for presenting here two simple figures, which recall in an intuitive way some of the geometrical characteristics of our *Frozen Waves*:

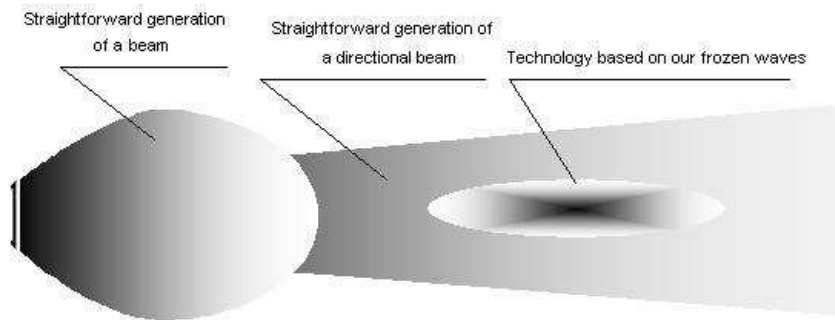


Figure 10: See the explications contained in the figures themselves, which apparently refer to: (a) ordinary (electromagnetic or acoustical) transmission; (b) standard directional transmission; and (c) well-localized transmission allowed by our Frozen Wave techniques. [Courtesy of Andrei Utkin]

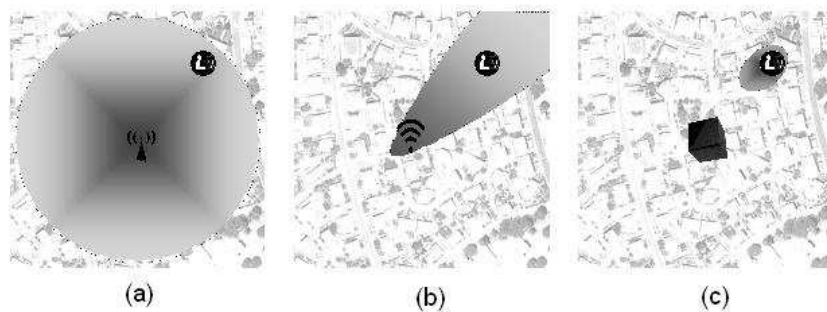


Figure 11: Areas covered by the electromagnetic (or acoustic) signals in the case, once more, of: (a) omnidirectional transmission; (b) standard directional transmission; and (c) spot-to-spot signal transmission permitted by our Frozen Wave techniques. [Courtesy of Andrei Utkin]

It may be stressed that the present (second) method, without any need of the paraxial approximation, does yield *exact* expressions for (well localized) beams with sizes *of the order* of their wavelength. It may be noticed, moreover, that the already-known exact solutions —for instance, the Bessel beams— are nothing but particular cases of solution (85).

An example: On choosing (with $0 \leq q_- < q_+ \leq 1$) the spectral double-step function

$$S(k_z) = \begin{cases} \frac{c}{\omega_0(q_+ - q_-)} & \text{for } q_- \omega_0/c \leq k_z \leq q_+ \omega_0/c \\ 0 & \text{elsewhere ,} \end{cases} \quad (86)$$

the coefficients of Eq.(85) become

$$A_n = \frac{ic}{2\pi n \omega_0 (q_+ - q_-)} \left[e^{-iq_+ \pi n} - e^{-iq_- \pi n} \right]. \quad (87)$$

The double-step spectrum (86) corresponds, with regard to the longitudinal wave number, to the mean value $\bar{k}_z = \omega_0(q_+ + q_-)/2c$ and to the width $\Delta k_z = \omega_0(q_+ - q_-)/c$. From such relations, it follows that $\Delta k_z/\bar{k}_z = 2(q_+ - q_-)/(q_+ + q_-)$.

For values of q_- and q_+ that do not satisfy the inequality $\Delta k_z/\bar{k}_z \ll 1$, the resulting solution will be a *non-paraxial* beam.

An exact solution can be found in Figure 38 of [11], which describes a beam with a spot diameter of $0.6 \mu\text{m}$ (for $\lambda_0 = 1 \mu\text{m}$) and, moreover, with a rather good longitudinal localization. In the case considered therein, about 21 terms in the sum entering Eq.(83) resulted to be quite enough for a good evaluation of the series. Such a beam was highly non-paraxial (having $\Delta k_z/\bar{k}_z = 1$), and therefore could not have been obtained by ordinary gaussian beam solutions, which are valid in the paraxial regime only. Notice that, for simplicity, we are referring ourselves to scalar wave fields only; but, in the case of non-paraxial optical beams, the vector character of the field has to be taken into account.

6.1 A new approach to the *Frozen Waves*

A noticeable property of our present method is that it allows a spatial modeling even of monochromatic fields (that correspond to envelopes *at rest*; so that, in the electromagnetic cases, one can speak, e.g., of the modeling of “light-fields at rest”). Let us repeat that such a modeling —rather interesting, especially for applications[8]— was already performed in Refs.[6, 4, 5], in terms of discrete superpositions of Bessel beams.

But the method presented in the last Section allows us to make use of *continuous* superpositions, in order to get a predetermined longitudinal (on-axis) intensity pattern, inside a desired space interval $0 < z < L$. Such continuous superposition writes[11, 4]

$$\Psi(\rho, z, t) = e^{-i\omega_0 t} \int_{-\omega_0/c}^{\omega_0/c} dk_z S(k_z) J_0(\rho k_\rho) e^{izk_z}, \quad (88)$$

which is nothing but the previous Eq.(72) with $v = 0$ (and therefore $\zeta = z$). In other words, Eq.(88) does just represent a *null-speed* subluminal wave. The FWs were expressed in the past as discrete superpositions, because it was not known at that time how to treat analytically a continuous superposition like (88). We are now able, however, to deal also with integrals: without numerical simulations, as we said, but in terms once more of analytic solutions.

Indeed, the exact solution of Eq.(88) is given by Eq.(85), with coefficients (83'); and one can choose the spectral function $S(k_z)$ in such a way that Ψ assumes the on-axis pre-chosen static intensity pattern $|F(z)|^2$. Namely, the equation to be satisfied by $S(k_z)$, to such an aim, is derived by associating Eq.(88) with the requirement $|\Psi(\rho = 0, z, t)|^2 = |F(z)|^2$, which entails the integral relation

$$\int_{-\omega_0/c}^{\omega_0/c} dk_z S(k_z) e^{izk_z} = F(z). \quad (89)$$

Equation (89) would be trivially solvable in the case of an integration between $-\infty$ and $+\infty$, since it would merely be a Fourier transformation; but obviously this is not the case, because its integration limits are finite. Actually, there are functions $F(z)$ for which Eq.(89) is not solvable at all, in the sense that no spectra $S(k_z)$ exist obeying the last equation. For instance, if we consider the *Fourier* expansion

$$F(z) = \int_{-\infty}^{\infty} dk_z \tilde{S}(k_z) e^{izk_z},$$

when $\tilde{S}(k_z)$ does assume non-negligible values outside the interval $-\omega_0/c < k_z < \omega_0/c$, then in Eq.(89) *no* $S(k_z)$ can forward that particular $F(z)$ as a result.

However, some procedures can be devised, such that one can nevertheless find out a function $S(k_z)$ that approximately (but satisfactorily) complies with Eq.(89).

The first procedure consists of writing $S(k_z)$ in the form

$$S(k_z) = \frac{1}{K} \sum_{n=-\infty}^{\infty} F\left(\frac{2n\pi}{K}\right) e^{-i2n\pi k_z/K}, \quad (90)$$

where, as before, $K = 2\omega_0/c$. Then, Eq.(90) can be easily verify as guaranteeing that the integral in Eq.(89) yields the values of the desired $F(z)$ *at the discrete points* $z = 2n\pi/K$. Indeed, the Fourier expansion (90) is already of the same type as Eq.(82), so that in this case the coefficients A_n of our solution (85), appearing in Eq.(83'), do simply become

$$A_n = \frac{1}{K} F\left(-\frac{2n\pi}{K}\right). \quad (91)$$

This is a powerful way for obtaining a desired longitudinal (on-axis) intensity pattern, especially for tiny spatial regions, because it is not necessary to solve any integral to find out the coefficients A_n , which by contrast are given directly by Eq.(91).

Figures 12 depict some interesting applications of this method. A few desired longitudinal intensity patterns $|F(z)|^2$ have been chosen, and the corresponding Frozen Waves calculated by using Eq.(85) with the coefficients A_n given in Eq.(91). The desired patterns are enforced to exist within very small spatial intervals only, in order to show the capability of the method to model[19] the field intensity shape also under such strict requirements.

In the four examples below, we considered a wavelength $\lambda = 0.6 \mu\text{m}$, which corresponds to $\omega_0 = b = 3.14 \times 10^{15}$ Hz. Details can be found in [11] The first longitudinal (on-axis) pattern considered by us is $F(z) = \exp[a(z - Z)]$ for $0 \leq z \leq Z$, and zero elsewhere; that is a pattern with an exponential increase, starting from $z = 0$ until $Z = 10 \mu\text{m}$ and with $a = 3/Z$. The intensity of the corresponding Frozen Wave is shown in Fig.12a.

The second longitudinal pattern (on-axis) taken into consideration is the gaussian one, given by $F(z) = \exp[-q(z/Z)^2]$ for $-Z \leq z \leq Z$, and zero elsewhere, with $q = 2$ and $Z = 1.6 \mu\text{m}$. The intensity of the corresponding Frozen Wave is shown in Fig.12b.

In the third example, the desired longitudinal pattern is supposed to be a super-gaussian, $F(z) = \exp[-q(z/Z)^{2m}]$ for $-Z \leq z \leq Z$, and zero elsewhere, where m controls the edge sharpness. We choose $q = 2$, $m = 4$ and $Z = 2 \mu\text{m}$. The intensity of the Frozen Wave obtained in this case is shown in Fig.12c.

Finally, in the fourth example, let us choose the longitudinal pattern as being the zero-order Bessel function $F(z) = J_0(qz)$ for $-Z \leq z \leq Z$, and zero elsewhere, with $q = 1.6 \times 10^6 \text{ m}^{-1}$ and $Z = 15 \mu\text{m}$. The intensity of the corresponding Frozen Wave is shown in Fig.12d.

Any static envelopes of this type can be easily transformed into propagating pulses by the mere application of Lorentz transformations (LT).

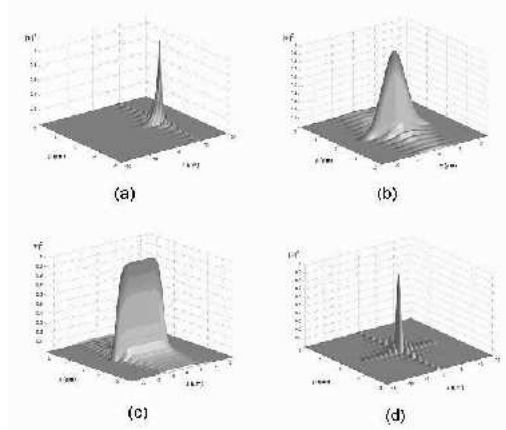


Figure 12: Frozen Waves with the on-axis longitudinal field pattern chosen as: **(a)** Exponential; **(b)** Gaussian; **(c)** Super-gaussian; **(d)** Zero order Bessel function

Another procedure exists for evaluating $S(k_z)$, based on the assumption that $S(k_z) \simeq \tilde{S}(k_z)$, which constitutes a good approximation whenever $\tilde{S}(k_z)$ assumes *negligible* values outside the interval $[-\omega_0/c, \omega_0/c]$. In such a case, one can have recourse to the method associated with Eq.(77) and expand $\tilde{S}(k_z)$ itself in a Fourier series, getting eventually the relevant coefficients A_n by Eq.(78). Let us recall that it is still $K \equiv k_{z\text{max}} - k_{z\text{min}} = 2\omega_0/c$.

It is worthwhile to call attention to the circumstance that, when constructing FWs in terms of a sum of discrete superpositions of Bessel beams (as it has been done in Refs.[6, 4, 5, 12, 8]), it was easy to obtain extended envelopes like, e.g., “cigars”: Where “easy” means by using only a few few terms of the sum. By contrast, when we construct FWs —following this Section— as continuous superpositions, then it is easy to get highly

localized (concentrated) envelopes. Let us explicitly mention, moreover, that the method presented in this Section furnishes FWs that are no longer periodic along the z -axis (a situation that, with our old method[6, 4, 5, 12], was obtainable only when the periodicity interval tended to infinity).

6.2 Frozen Waves in absorbing media

Let us mention that it is possible to obtain even in *absorbing media* non-diffracting “*stationary*” wave fields capable to assume, approximately, any desired longitudinal intensity pattern within a chosen interval $0 \leq z \leq L$ of the propagation axis z . These new solutions are more easily realizable in practice, at the extent to be more indicated for the various applications already mentioned by us.

We know that, when propagating in a non-absorbing medium, the NDWs[6, 4] maintain their spatial shape for long distances. The situation is not the same when dealing with absorbing media: In such cases, both the ordinary and the non-diffracting beams (and pulses) will be exponentially attenuated along the propagation axis.

It can be however shown that, through suitable superpositions of equal-frequency Bessel beams, it is possible to obtain non-diffracting beams *in absorbing media*, whose longitudinal intensity pattern can assume any desired shape within a chosen interval $0 \leq z \leq L$ of the propagation axis z . For example, one can obtain non-diffracting beams capable to resist the loss effects, maintaining amplitude and spot size of their central core for long distances.

The corresponding method, with some interesting examples, is expounded in Ref.[5] and in Chapter 2 of [1]

6.3 Experimental production of the Frozen Waves

Frozen Waves have been eventually produced, in recent times[109], in Optics, as reported also in another Chapter of this Volume; while we expect their production also in Acoustics, even if till the present moment only simulated experiments have been performed[7].

7 On The role of Special Relativity, and of Lorentz Transformations

Strict connections exist between, on one hand, the principles and structure of Special Relativity and, on the other hand, the whole subject of subluminal, luminal, Superluminal Localized Waves, and it is expected since long time that a priori they are transformable one into the other via suitable Lorentz transformations (cf. Refs.[92, 110, 111, 112, 113, 114, 115, 116]).

Let us first confine ourselves to the cases faced in this last Sections. Our subluminal localized pulses, that may be called “wave bullets”, behave as *particles*: Indeed, our subluminal pulses [as well as the luminal and Superluminal (X-shaped) ones, that have been so amply investigated in the past literature] do exist as solutions of any wave equations, ranging from electromagnetism and acoustics or geophysics, to elementary particle physics (and even, as we discovered recently, to gravitation physics). From the kinematical point of view, the velocity composition relativistic law holds also for them. The same is true, more in general, for any localized waves (pulses or beams).

Let us start for simplicity by considering, in an initial reference-frame O, just a (ν -order) Bessel beam $\Psi(\rho, \phi, z, t) = J_\nu(\rho k_\rho) e^{i\nu\phi} e^{izk_z} e^{-i\omega t}$. In a second reference-frame O', moving with respect to (w.r.t.) O with speed u —along the positive z-axis and in the positive direction, for simplicity's sake—, it will be observed[116] the new Bessel beam

$$\Psi(\rho', \phi', z', t') = J_\nu(\rho' k'_{\rho'}) e^{i\nu\phi'} e^{iz'k'_{z'}} e^{-i\omega' t'} , \quad (80)$$

obtained by applying the appropriate Lorentz transformation (a Lorentz “boost”) with $\gamma = [\sqrt{1 - u^2/c^2}]^{-1}$, and $k'_{\rho'} = k_\rho$; $k'_{z'} = \gamma(k_z - u\omega/c^2)$; $\omega' = \gamma(\omega - uk_z)$; this can be easily seen, e.g., by putting $\rho = \rho'$; $z = \gamma(z' + ut')$; $t = \gamma(t' + uz'/c^2)$ directly into Eq.(80).

Let us now pass to subluminal *pulses*. We can investigate the action of a Lorentz transformation (LT), by expressing them either via the first method, or via the second one, of our Section 5. Let us consider for instance, in the frame O, a v -speed (subluminal) pulse[11] given in our Section 5. When we go on to a second observer O' moving *with the same speed* v w.r.t. frame O, and, still for the sake of simplicity, passing through the origin O of the initial frame at time $t = 0$, the new observer O' will see the pulse[116]

$$\Psi(\rho', z', t') = e^{-it'\omega'_0} \int_{\omega_-}^{\omega_+} d\omega S(\omega) J_0(\rho' k'_{\rho'}) e^{iz'k'_{z'}} , \quad (81)$$

with $k'_{z'} = \gamma^{-1}\omega/v - \gamma b/v$; $\omega' = \gamma b = \omega'_0$; $k'_{\rho'} = \omega'_0/c^2 - k'_{z'}{}^2$, as one gets from the mentioned Lorentz boost[11], with $u = v$ (and γ defined as usual[11]). Notice that $k'_{z'}$ is a function of ω ; and that here ω' is a constant.

If we explicitly insert into Eq.(81) the relation $\omega = \gamma(vk'_{z'} + \gamma b)$, which is nothing but a re-writing of the first one of the relations following Eq.(81) above, then Eq.(81) becomes[116]

$$\Psi(\rho', z', t') = \gamma v e^{-it'\omega_0} \int_{-\omega_0/c}^{\omega_0/c} dk'_{z'} \bar{S}(k'_{z'}) J_0(\rho' k'_{\rho'}) e^{iz'k'_{z'}} , \quad (82)$$

where \bar{S} is expressed in terms of the previous function $S(\omega)$, entering Eq.(81), as follows: $\bar{S}(k'_{z'}) = S(\gamma vk'_{z'} + \gamma^2 b)$. Equation (82) describes monochromatic beams with axial symmetry (and does coincide also with what derived within our second method, in Section 5, when posing $v = 0$).

The conclusion is that a subluminal pulse, given by our Eq.(57), which appears as a v -speed *pulse* in a frame O, will appear[116] in another frame O' (traveling w.r.t. observer O with the same speed v in the same direction z) just as the *monochromatic beam* in Eq.(82) endowed with angular frequency $\omega'_0 = \gamma b$, whatever be the pulse spectral function in the initial frame O: even if the kind of monochromatic beam, one arrives to, does of course depend on the chosen $S(\omega)$. The vice-versa is also true, in general. [Notice, incidentally, that one gets in particular a Bessel-type beam when S is a Dirac's delta-function: $S(\omega) = \delta(\omega - \omega_0)$; moreover, let us notice that, on applying a LT to a Bessel beam, one obtains another Bessel beam, with a different axicon-angle]. Let us set forth explicitly an observation that up to now has been noticed only in Ref.[19]. Namely, let us mention that, when starting not from Eq.(57) but from the most general solutions which—as we have already seen—are *sums* of solutions (57) over the various values b_m of b , then a Lorentz transformation will lead us to *a sum* of monochromatic beams: actually, of harmonics (rather than to a single monochromatic beam). In particular, if one wants to obtain a sum of harmonic beams, one has to apply a LT to more general subluminal pulses.

Let us add that *also* the various Superluminal localized pulses get transformed[116] one into the other by the mere application of ordinary LTs; while it may be expected that the subluminal and the Superluminal NDWs are to be linked (apart from some known technical difficulties, that require a particular caution[37]) by the Superluminal Lorentz “transformations” expounded long ago, e.g., in Refs.[110, 111, 115, 92] and refs. therein. Let us recall at this point that, in the years 1980-82, special relativity, in its non-restricted version, predicted that, while the *simplest* subluminal *object* is obviously a sphere (or, in the limit, a space point), the simplest Superluminal object is on the contrary an X-shaped pulse (or, in the limit, a double cone): This is shown in Fig.13. The circumstance that the localized solutions to the *wave equations* follow indeed the same pattern is rather interesting, and might be of help—in the case, e.g., of elementary particles and quantum physics—for a deeper comprehension of de Broglie's and Schroedinger's wave mechanics, and of the corpuscle/wave duality. With regard to the fact that the *simplest* subluminal NDWs, solutions to the wave equation, are “ball-like”, let us present in Figs.14, in ordinary 3D space, the general shape of the simple Mackinnon's solutions, as expressed by Eq.(63) for $v \ll c$: In such figures we graphically depict the field iso-intensity surfaces, which (as expected) result to be just spherical in the considered case.

We have also seen, among the others, that, even if our first method (subsection 5.1) cannot *directly* yield zero-speed envelopes, such envelopes “at rest”, Eq.(85), can be however obtained by applying a v -speed LT to Eq.(130). In this way, one starts from many frequencies [Eq.(69)] and ends up with one frequency only [Eq.(85)], since b gets transformed into *the* frequency of the monochromatic beam. Let us add a warning: The topic of Superluminal LTs is a delicate one[110, 111, 115, 92], at the extent that the majority of the recent attempts to re-address this question and its applications (cf., e.g., Ref.[37] and references therein) risk to be defective: in some cases they did not even respect the necessary covariance of the wave equation itself.

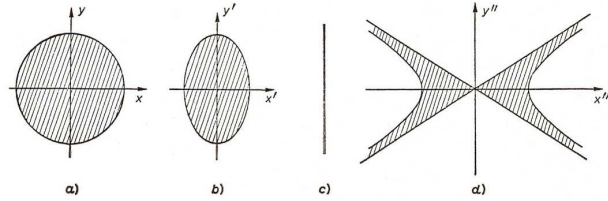


Figure 13: From *Non-restricted special Relativity*, also called “Extended special Relativity” [37, 110] one can recall the following. An intrinsically spherical (or pointlike, at the limit) object appears in the vacuum as an ellipsoid contracted along the motion direction when endowed with a speed $v < c$. By contrast, if endowed with a speed $V > c$ (even if the c -speed barrier cannot be crossed, neither from the left nor from the right), it would appear [92, 110, 37] no longer as a particle, but as occupying the region delimited by a double cone and a two-sheeted hyperboloid —or as a double cone, at the limit—, and moving with Superluminal speed V [the cotangent square of the cone semi-angle, with $c = 1$, being $V^2 - 1$. For simplicity, a space axis is skipped. This figure is taken from our Refs. [92, 110]. It is remarkable that the shape of the localized (subluminal and Superluminal) pulses, solutions to the *wave equations*, appears to follow the same behaviour; this can have a role for a better comprehension even of the corpuscle/wave duality, that is, of de Broglie and Schroedinger wave-mechanics. See also Fig.14.

Further details on these topics can be found in Refs. [11, 1, 13, 14], where, in connection with the fact that the X-shaped pulses are endowed with Superluminal peak-velocities, an overview was presented of the various experimental sectors of physics in which superluminal motions do seem to appear. Namely, also a bird’s-eye view was given therein of the *experiments* till now performed with evanescent waves (and/or tunneling photons), and with the NDW solutions to the wave equations.

8 Non-axially symmetric solutions: The case of higher-order Bessel beams

Let us stress that till now we paid attention to exact solutions representing axially-symmetric (subluminal) pulses only: that is to say, to pulses obtained by suitable superpositions of zero-order Bessel beams.

It is however interesting to look also for analytic solutions representing *non*-axially symmetric subluminal pulses, which can be constructed in terms of superpositions of ν -order Bessel beams, with ν a positive integer ($\nu > 0$). This can be attempted both in the case of subsection 5.1 (first method), and in the case of Sect.5.3 (second method). For brevity’s sake, let us take only the first method (subsection 5.1) into consideration.

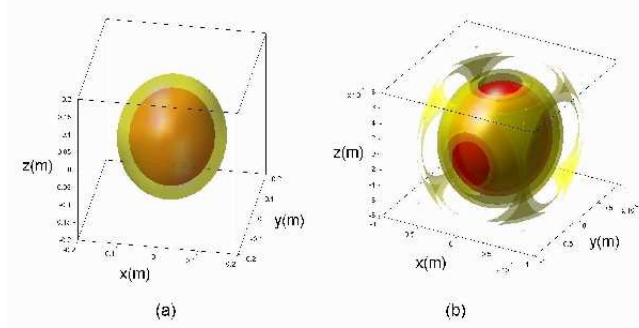


Figure 14: In the previous figure we have seen how SR, in its non-restricted version (NRR), predicted[92, 110] that, while the *simplest* subluminal object is obviously a sphere (or, in the limit, a space point), the simplest Superluminal object is on the contrary an X-shaped pulse (or, in the limit, a double cone). The circumstance that the Localized Solutions to the *wave equations* do follow the same pattern is rather interesting, and is expected to be useful—in the case, e.g., of elementary particles and quantum physics—for a deeper comprehension of de Broglie’s and Schroedinger’s wave mechanics. With regard to the fact that the *simplest* subluminal NDWs, solutions to the wave equations, are “ball-like”, let us depict by these figures, in the ordinary 3D space, the general shape of the Mackinnon’s solutions as expressed by Eq.(124), numerically evaluated for $v \ll c$. In figures (a) and (b) we graphically represent the field iso-intensity surfaces, which in the considered case result to be (as expected) just spherical.

One is immediately confronted with the difficulty that *no* exact solutions are known for the integral in Eq.(62) when $J_0(\cdot)$ is replaced with $J_\nu(\cdot)$. One can overcome this difficulty by following a simple method, which allows obtaining “higher-order” subluminal waves in terms of the axially-symmetric ones. Indeed, it is well-known that, if $\Psi(x, y, z, t)$ is an exact solution to the ordinary wave equation, then $\partial\Psi/\partial x$ and $\partial\Psi/\partial y$ are also exact solutions [incidentally, even $\partial^n\Psi/\partial z^n$ and $\partial^n\Psi/\partial t^n$ will be exact solutions]. By contrast, when working in cylindrical co-ordinates, if $\Psi(\rho, \phi, z, t)$ is a solution to the wave equation, quantities $\partial\Psi/\partial\rho$ and $\partial\Psi/\partial\phi$ are *not* solutions, in general. Nevertheless, it is not difficult at all to reach the noticeable conclusion that, once $\Psi(\rho, \phi, z, t)$ is a solution, then also

$$\bar{\Psi}(\rho, \phi, z, t) = e^{i\phi} \left(\frac{\partial\Psi}{\partial\rho} + \frac{i}{\rho} \frac{\partial\Psi}{\partial\phi} \right) \quad (83)$$

is an exact solution! For instance, for an axially-symmetric solution of the type $\Psi = J_0(k_\rho\rho) \exp[ik_z z] \exp[-i\omega t]$, equation (83) yields $\bar{\Psi} = -k_\rho J_1(k_\rho\rho) \exp[i\phi] \exp[ik_z z] \exp[-i\omega t]$, which is actually one more analytic solution. In other words, it is enough to start for simplicity from a zero-order Bessel beam, and to apply Eq.(83), successively, ν times, in order to get as a new solution

$\bar{\Psi} = (-k_\rho)^\nu J_\nu(k_\rho \rho) \exp[i\nu\phi] \exp[ik_z z] \exp[-i\omega t]$, which is a ν -order Bessel beam.

In such a way, when applying ν times Eq.(83) to the (axially-symmetric) subluminal solution $\Psi(\rho, z, t)$ in Eqs.(69,68,67) [obtained from Eq.(57) with spectral function $S(\omega)$], we get the subluminal non-axially symmetric pulses $\Psi_\nu(\rho, \phi, z, t)$ as new analytic solutions, consisting as expected in superpositions of ν -order Bessel beams:

$$\Psi_n(\rho, \phi, z, t) = \int_{\omega_-}^{\omega_+} d\omega S'(\omega) J_\nu(k_\rho \rho) e^{i\nu\phi} e^{ik_z z} e^{-i\omega t}, \quad (84)$$

where $k_\rho(\omega)$ is given by Eq.(58), and quantities $S'(\omega) = (-k_\rho(\omega))^\nu S(\omega)$ are the spectra of the new pulses. If $S(\omega)$ is centered at a certain carrier frequency (it is a gaussian spectrum, for instance), then $S'(\omega)$ too will approximately result to be of the same type.

Now, if we wish the new solution $\Psi_\nu(\rho, \phi, z, t)$ to possess a pre-defined spectrum $S'(\omega) = F(\omega)$, we can first take Eq.(57) and put $S(\omega) = F(\omega)/(-k_\rho(\omega))^\nu$ in its solution (69), and afterwards apply to it, ν times, the operator $U \equiv \exp[i\phi] [\partial/\partial\rho + (i/\rho)\partial/\partial\phi]$: As a result, we will obtain the desired pulse, $\Psi_\nu(\rho, \phi, z, t)$, endowed with $S'(\omega) = F(\omega)$.

An example — On starting from the subluminal axially-symmetric pulse $\Psi(\rho, z, t)$, given by Eq.(69) with the *gaussian* spectrum (70), we can get the subluminal, non-axially symmetric, exact solution $\Psi_1(\rho, \phi, z, t)$ by simply calculating

$$\Psi_1(\rho, \phi, z, t) = \frac{\partial\Psi}{\partial\rho} e^{i\phi}, \quad (85)$$

which actually yields the “first-order” pulse $\Psi_1(\rho, \phi, z, t)$, which can be more compactly written in the form:

$$\Psi_1(\rho, \phi, \eta, \zeta) = 2\frac{b}{c}v\gamma^2 \exp\left[i\frac{b}{c}\beta\gamma^2\eta\right] \sum_{n=-\infty}^{\infty} A_n \exp[in\frac{\pi}{\beta}] \psi_{1n} \quad (86)$$

with

$$\psi_{1n}(\rho, \phi, \eta, \zeta) \equiv \frac{b^2}{c^2} \gamma^2 \rho Z^{-3} [Z \cos Z - \sin Z] e^{i\phi}, \quad (87)$$

where

$$Z \equiv \sqrt{\frac{b^2}{c^2} \gamma^2 \rho^2 + \left(\frac{b}{c} \gamma^2 \zeta + n\pi\right)^2}. \quad (88)$$

This exact solution, let us repeat, corresponds to superposition (84), with $S'(\omega) = k_\rho(\omega)S(\omega)$, quantity $S(\omega)$ being given by Eq.(70). It is represented in Figure 15. The *pulse* intensity has a “donut-like” shape.

Let us take the liberty of recalling that in Chap.2 of [1], in connection with the *frozen waves*, we argued about the possibility of increasing even more our control on their transverse shape also by using higher-order Bessel beams in the FWs fundamental superposition Eq.(2.74) in [1]. That new approach can be understood and accepted on the basis of simple and intuitive arguments, which can be found in Ref.[12].

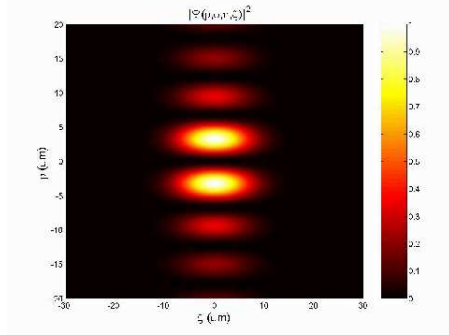


Figure 15: Orthogonal projection of the field intensity corresponding to the higher order subluminal *pulse* represented by the exact solution Eq.(85), quantity Ψ being given by Eq.(69) with the gaussian spectrum (70). The pulse intensity happens to have this time a “donut”-like shape.

In the mentioned Chap.2 of [1] we showed for example how to obtain a *cylindrical surface of “static” light*, in correspondence with a chosen space interval $0 \leq z \leq L$ (for instance, with $L = 238 \mu\text{m}$).

Figure 16 depicts the longitudinal intensity pattern as it was approximately obtained, shifted from $\rho = 0$ to a different value of ρ (in this case, $\rho = 7.75 \mu\text{m}$). The resulting field resembles indeed a cylindrical surface of “static” light with radius $7.75 \mu\text{m}$ and length $238 \mu\text{m}$.

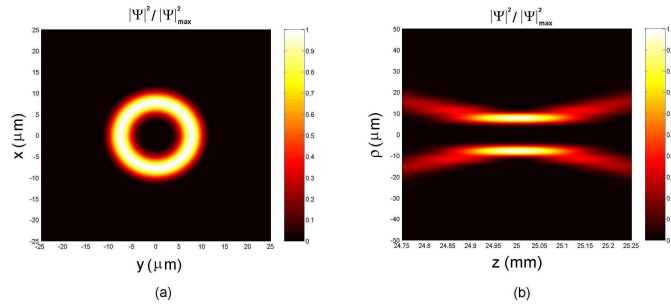


Figure 16: **(a)** Transverse section at $z = L/2$ of the considered higher-order Frozen Wave. **(b)** Orthogonal projection of the three-dimensional intensity pattern of the same higher-order FW. The resulting field resembles indeed a cylindrical surface of “static” light with the chosen radius $7.75 \mu\text{m}$ (and the chosen length $238 \mu\text{m}$).

9 An Application to Biomedical Optics: NDWs and the “GLMT” (Generalized Lorenz-Mie Theory)

We mentioned above in several places the possible applications of NDWs, quoting even a patent of ours[8] regarding the FWs. Let us exploit here at least the theoretical aspects of an application in biomedical optics.

As we know, NDWs have become a hot topic nowadays in a variety of fields. Let us recall in particular that their use, replacing laser beams for achieving multiple traps, has found many potential applications in medicine and biomedicine[117, 118, 119, 120, 121]. Even though their multi-ringed structure is not suitable for an effective three-dimensional trap when single beam setups are employed, nevertheless, with today techniques for their generation and real-time control, non-diffracting beams have become (better than focused Gaussian beams or others), indispensable “laser-type” beams for biological studies by means of optical tweezing and micromanipulation techniques.

The theory involved in optical trapping and micro manipulation (for a review see, e.g., Ref.[122]) is strongly dependent upon the relative size and electromagnetic parameters of the scatterer, which is in general assumed to have some symmetric shape (sphere, cylinder, ellipsis,...). If we take the electromagnetic properties of the particle and of the surrounding medium to be of the same order (as it usually happens for biological particles immersed in water or oil), two situations are of particular theoretical interest, related with the possibility of avoiding, or just eliminating, too large an amount of algebra or numerical calculations.

The first one is met when the size parameter s of the scatterer is much larger than the wavelength λ of the wave ($s \gg \lambda$), so that geometrical optics considerations become the fastest and most convenient way to find out the physical properties of interest[121, 123, 124, 125].

The second one, on the contrary, concerns very small particles: that is, scatterers whose overall dimension may be considered a small fraction of the wavelength ($s \ll \lambda$), so that the Rayleigh theory becomes the most suitable theoretical approach for solving the associated scattering problem [126]. Indeed, both the ray optics method and the Rayleigh theory are extremely accurate within their range of validity and remain valid for any incident wave (as long as it is adequately modeled).

However, for s close to 1, it results to be difficult to formulate analytic closed-form expressions for the physical properties of interest. In this particular situation, indeed, none of the two aforementioned approaches is of any help, and one is forced to adopt alternative approaches or techniques, such as the so-called Lorenz-Mie theory (for plane waves and spherical particles) or its generalized version, the GLMT (Generalized Lorenz-Mie Theory)[127, 128, 129, 130] for arbitrary wave fields. We adopt the GLMT in this Section mainly because it seems to be the most established numerical/theoretical formalism for arbitrary-size particles in scattering problems (for further methods see, for instance, Ref.[131] and references therein).

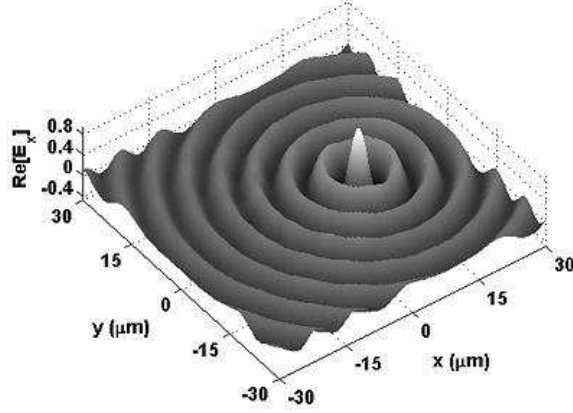


Figure 17: The E_x component generated by the “GLMT” for an ordinary Bessel beam (BB) with $\lambda = 532\mu\text{m}$. The axicon angle θ_a was chosen to be 5° , a limiting number for which the paraxial approximation may still be considered valid.

In the framework of the GLMT and for spherical scatterers, a v -th order paraxial Bessel beam

$$\psi = J_v(k_\rho \rho) \exp(i\omega t) \exp(iv\phi) \quad (89)$$

must be described in terms of the beam-shape coefficients (BSCs) $g_{n,TM}^m$ and $g_{n,TE}^m$ (n, m being integers), because of the mathematical structure commonly used for the incident electromagnetic field (which is based on power series expansions in terms of vector spherical harmonics[131]). The BSCs are, thus, the coefficients of such expansion, and are responsible for an adequate description of the spatial intensity profile of the wave.

Much effort has been devoted during the last years in order to get reliable and useful descriptions of scalar Bessel beams, envisioning optical trapping and micro manipulation, particle sizing applications and so on. In fact, if the radial component of the electric field, E_r , is given, or known, then the BSCs $g_{n,TM}^m$ will read[131], in a spherical coordinate system whose origin coincides with the center of the particle, as:

$$g_{n,TM}^m = \frac{(2n+1)^2}{2\pi^2 n(n+1) c_n^{pw}} \frac{(n-|m|)!}{(n+|m|)!} \int_0^{2\pi} \int_0^\pi \int_0^\infty \frac{E_r(r, \theta, \phi)}{E_0} r \Psi_n^{(1)}(kr) \times \quad (90)$$

$$\times P_n^{|m|}(\cos\theta) \exp(-im\phi) \sin\theta d(kr) d\theta d\phi,$$

or

$$g_{n, TM}^m = \frac{2n+1}{4\pi n(n+1)c_n^{pw}} \frac{(n-|m|)!}{(n+|m|)!} \frac{a}{\Psi_n^{(1)}(ka)} \int_0^{2\pi} \int_0^\pi \frac{E_r(r=a, \theta, \phi)}{E_0} \times \quad (91)$$

$$\times P_n^{|m|}(\cos\theta) \exp(-im\phi) \sin\theta \, d\theta \, d\phi ,$$

where Eq.(91) follows from a suitable choice of the spatial parameter a . In the above expressions, $c_n^{pw} = (-i)^{n+1}(2n+1)/(kn(n+1))$, while k is the wave number in the external medium, and the $\Psi_n^{(1)}$ are spherical Bessel functions; at last, quantities $P_n^{|m|}(\cos\theta)$ are the associated Legendre polynomials, and E_0 the electric field strength. The coefficients $g_{n, TE}^m$ follow from similar considerations.

Unless Eq.(90) or Eq.(91) are numerically evaluated, they a priori give us no direct insight on the behavior of the beam shape coefficients $g_{n, TM}^m$ and $g_{n, TE}^m$, which may be, or may not be, written in terms of any of the following parameters, or values: n , m , the size-parameter s , the *spot* $\Delta\rho$ of the impinging Bessel beam, and the perpendicular distance ρ_0 between the optical axis of the beam and the center of the particle. Several researchers have devoted time to the derivation of numerically efficient and fast computing techniques and formulae, instead of simply implementing recursive algorithms for computing triple and double integrations as given by (90) and (91), respectively[132, 133, 134, 135, 136].

We have recently shown that, in spherical coordinates, a scalar ordinary Bessel beam (BB) can be accurately described by means of what has been called[137] the Integral Localized Approximation (ILA), a method that considerably revolutionized the numerical aspects of the generalized Lorenz-Mie theory, by making it possible to obtain, in a numerically-efficient way, closed-form expressions[132, 133, 134, 135, 136, 137, 138] for the BSCs. For example, a zero order Bessel beam (BB) propagating along his axiz z and polarized along x , when displaced along the x direction of a distance $\rho_0 = x_0$, has its BSCs, $g_{n, TM}^m$ and $g_{n, TE}^m$, given by the simple expressions[137]:

$$g_{n, TM}^0 = i \frac{2n(n+1)}{2n+1} J_1(\varpi) J_1(\xi) \exp(ik_z z_0) \quad (92)$$

$$g_{n, TM}^{m \neq 0} = \frac{1}{2} \left(\frac{-2i}{2n+1} \right)^{|m|-1} \times \quad (93)$$

$$\times \left[J_{|m|-1}(\varpi) J_{|m|-1}(\xi) + J_{|m|+1}(\varpi) J_{|m|+1}(\xi) \right] \exp(ik_z z_0) ,$$

$$g_{n, TE}^0 = 0 \quad (94)$$

$$g_{n, TE}^{\pm|m| \neq 0} = \frac{\mp i}{2} \left(\frac{-2i}{2n+1} \right)^{|m|-1} \times \quad (95)$$

$$\times \left[J_{|m|-1}(\varpi) J_{|m|-1}(\xi) - J_{|m|+1}(\varpi) J_{|m|+1}(\xi) \right] \exp(ik_z z_0) ,$$

quantity k_z being the longitudinal wave number, z_0 a constant which accounts for the correct phase of the wave at some observation point, $\varpi = (n + 1/2) \sin\theta_a$, and $\xi = x_0 k \sin\theta_a$ (θ_a being the axicon angle). Once the BSCs have been found, all the EM field components can be readily obtained by using double summation expressions[131]. For instance, E_r reads

$$E_r(r, \theta, \phi) = -iE_0 \sum_{n=1}^{\infty} (-i)^n (2n + 1) \frac{\Psi_n^{(1)}(kr)}{kr} \sum_{m=-n}^n g_{n, TM}^m \pi_n^{|m|}(\theta) \sin\theta \exp(im\phi) \quad (96)$$

whose original value E_x is given by (96) when imposing $E_x = E_r(r = |x_0|, \theta = \pi/2, \phi = 0)$ for $x > 0$ and $E_x = E_r(r = |x_0|, \theta = \pi/2, \phi = \pi)$ for $x < 0$, as we have depicted in Fig.17. Unfortunately, the higher the radial displacement ρ_0 of the beam relative to the particle, the higher the number of BSCs that come into play in Eqs.(92-96), or, more generally, in the evaluation of all the physical properties of interest (radiation pressure cross-sections, torques, spatial intensity distribution, and so on). Nevertheless, the set of Eqs.(92-95) can speed-up numerical calculations by a factor of 100, or even 1,000, with respect to that expected from a direct use of (90) and (91) [137]. With such a fast computing technique, together with equivalent expressions for some other specific polarizations, there have been investigated some of the most fundamental trapping properties of (absorbent or lossless) arbitrary size spheres, simple or stratified, with positive or negative refractive indexes: The results being more or less in accordance with what should be expected in a real experiment[131, 137, 139, 140]. By “more or less” we mean that the ILA does not predict the changes in the intensity profile of the beam, after its passage through the lens system and the objective of the microscope... (a good theoretical approach to this case has been recently demonstrated for a focused Gaussian beam [141, 142]).

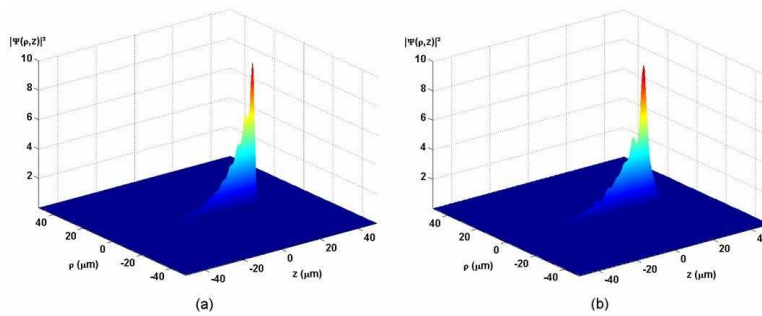


Figure 18: (a) A frozen wave with exponential growth, generated by the method in Ref.[90] through a superposition of Bessel beams, all with the same frequency $\omega = 6.12 \times 10^{15}$ Hz. (b) Same as (a), but now using the ILA for computing the BSCs of each Bessel beam.

The same approach was more recently applied for the BSCs of higher order Bessel beams, under the paraxial approximation, for studying the optical forces exerted over biological cells [140]. Even though the paraxial restriction may not be adequate in some cases, it allows one to rapidly evaluate the angular and linear momentum transfer characteristics for a wide range of spherical-like, simple or stratified structures and biological particles. Incidentally, if the beam is an authentic Maxwellian wave (which is not the case for a Gaussian beam), the ILA provides a fast and reliable alternative for investigating scattering problems within the GLMT. It should be emphasized that the formulation in Refs.[141, 142] leads to analytical BSC expressions similar to those given by Eqs.(92) and (93), thus demonstrating how close the ILA outputs are to the exact quadrature expressions, (90) and (91) or, equivalently, to what provided in Ref.[141].

One of the particularities of the GLMT is that, when the incident beam is replaced by another one with different parameter s , all subsequent formulae and numerical code remain unchanged, avoiding redefinition or inclusion of additional lines in the numerical algorithm which contains the expressions for the physical parameters to be calculated. Further, once the BSCs for a given BB are given, any impinging wave constructed by means of a suitable superposition of them can also be easily described and investigated. This is of great interest in the case of static (zero speed) longitudinal intensity patterns, generated by superposing N equal-frequency zero-order Bessel beams with different longitudinal wave number—which is the interesting case[4] of the Frozen Waves (FWs) [whose experimental production has been recently realized, let us repeat, for the case of longitudinal intervals of the order[109] of 1 m]. Notice that the BSCs of paraxial FWs would simply involve a summation of N individual BSCs, each one adequately weighted in order to model some pre-chosen longitudinal intensity pattern. This simple and direct technique enables the description of FWs for a large number of potential applications, as already said elsewhere. Figure 18 reveals, for example, the equivalent of the longitudinal exponential intensity pattern first introduced in Ref.[4] for mid-range purposes. It is clearly seen that, indeed, the GLMT is capable of handling this new class of “laser beams” and provide pretty good results for their associated optical properties, such as the longitudinal radiation pressure cross-section profile of Fig.18, as shown in Fig.19.

The transverse intensity control provided by the superposition of higher order BBs could also be taken into account by using the analytic expressions for the BSCs, provided, for example, in Ref.[140] for single BBs. Finally, future theoretical work may allow one to deal with both scalar and vector FWs, since it is understandable that, once an accurate description of arbitrary order scalar BBs is given, their equivalent vector fields are somehow functions of those same Bessel functions that enter into their expressions, and that can therefore be described by the GLMT in terms of their field components[121, 143].

Bessel beams have also been theoretically introduced as one of the first “laser beam” for studying the mechanical properties of simple negative refractive-index (NRI) scatterers [139, 89]. For such particles, the matching condition (that is, the identity of the impedance

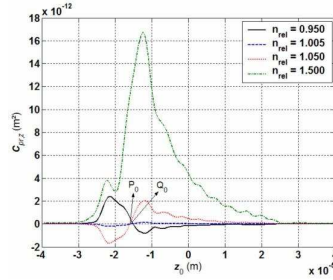


Figure 19: Radiation pressure cross-section exerted on a spherical dielectric particle of radius $a = 3.75\mu\text{m}$, as a function of its relative refractive index and of the distance z_0 from $z = 0$. The external medium is assumed to be water. Points of longitudinal stable equilibrium are denoted by P_0 and Q_0 .

of the external medium with that of the particle) is known to produce non-zero radial and scattering optical-forces, even if the wave suffers no reflection at the surface of the sphere, in contrast with the ordinary case of positive refractive index (PRI) particles[144, 145, 146]. Using Bessel beams (both in the ray optics and in the GLMT), it has been possible to show, for example, that a given NRI spherical particle can be radially either attracted by or repelled from the bright or dark annular intensity disks: This behavior being strongly affected by how the incident wave distributes itself in space, i.e., by its spot and relative transverse distance.

If the medium inside which the particle is embedded is lossy (or if the scatterer itself is absorber), it is also possible to conceive the incorporation of Diffraction-Attenuation Resistant Beams (DARBs) into some optical tweezers setup[5, 90], so that any pre-fixed longitudinal intensity provides the experimentalist with the expected optical properties. However, the generation and implementation of DARBs for arbitrary-range applications are still open problems.

10 Soliton-like solutions to the ordinary Schroedinger equation, within standard QM

As we know, not only nonlinear, but also a large class of linear equations (including the wave equations) admit of “soliton-like” solutions, which propagate without distortion in one direction. In the case of the (linear) wave equations, for such soliton-like solutions we have used the name of Non-diffracting Waves (NDW). It was soon thought that, since these solutions to the wave equations are non-diffractive and particle-like, they are a priori suitable, more than gaussian’s, for describing elementary particle motion, and may well be related their wave nature[35, 39]. In fact, localized solutions were soon found also

for Klein-Gordon and for Dirac equations[35, 39]. In this Section we show[3] that, *mutatis mutandis*, non-diffracting solutions exist even for the ordinary (linear) Schroedinger equation within standard Quantum Mechanics; were we may obtain both approximate and exact solutions. In the ideal case such solutions (even if localized, and "decaying") are not square-integrable, analogously to plane or spherical waves: one has to show therefore how to obtain finite-energy solutions. The approach can of course be extended also for a particle moving in the presence of a potential[3].

Little work[40] was done in the past for the case of the ordinary *Schroedinger* equation: see, e.g., besides [29], also Refs.[39]. Indeed, the Schroedinger case is different, since the relation between the energy E and the impulse magnitude $p \equiv |\mathbf{p}|$ is quadratic [$E = p^2/(2m)$] in non-relativistic cases, like in Schroedinger's, at variance with the relativistic ones. We might mention that many non-diffracting (especially X-shaped) solutions have been constructed for the linear[43] or nonlinear[44] equations that in Optics bear the name of "*Schroedinger equation*", even if they are mathematically very different from the ordinary Schroedinger's. Moreover, a special kind of non-diffracting packet solutions, in terms of Airy functions, were found in the seventies for the case of the actual 1D Schroedinger equation, and extended later on to the 3D case. All that has been recently applied to the case of Optics, originating the discovery of Airy-type waves, now well-known for their remarkable properties[147, 148, 149, 150, 151]: Such Airy waves being solutions, once more, to the so-called (linear) "Schroedinger equation" of Optics. But, as we were saying, the non-diffracting solutions to the ordinary Schroedinger equation, within standard Q.M., are quite apt themselves at describing elementary particles. They will result rather different from the ones found in Optics, both for the mentioned fact that the optical Schroedinger equation is mathematically different from the ordinary Schroedinger equation, and for the fact that our approach and methods are quite different from the ones adopted in Optics.

Before going on, let us first recall that in the time-independent realm —or, rather, when the dependence on time is only harmonic, i.e., for monochromatic solutions— the (quantum, non-relativistic) Schroedinger equation happens to be mathematically identical to the (classical, relativistic) Helmholtz equation[152, 153, 154, 155]. And many trains of localized X-shaped pulses have been found, as *superpositions* of solutions to the Helmholtz equation, which propagate, for instance, along cylindrical or co-axial waveguides[68]; but we shall skip all the cases[69, 70] of this type, since we are concerned here with propagation in free space, even when in the presence of an ordinary potential. Let us also mention that, in the general time-*dependent* case, that is, in the case of pulses, the Schroedinger and the ordinary wave equation are no longer mathematically identical, since the time derivative results to be of the first order in the former and of the second order in the latter. [It has been shown that, nevertheless, at least in some cases, they still share various classes of analogous solutions, differing only in their spreading properties[153]]. Moreover, the Schroedinger equation implies the existence of an *intrinsic* dispersion relation even for free particles; this is another difference to pay attention to: the solutions to the wave equation suffer only diffraction (and no dispersion) in the vacuum, while those of the Schroedinger

equation suffer also (an intrinsic) dispersion even in the vacuum.

10.1 Bessel *beams* as non-diffracting solutions (NDS) to the Schroedinger equation

Let us consider the Schroedinger equation for a free particle (an electron, for example)

$$\nabla^2\psi + \frac{2im}{\hbar} \frac{\partial\psi}{\partial t} = 0. \quad (97)$$

If we confine ourselves to solutions of the type

$$\psi(\rho, z, \varphi; t) = F(\rho, z, \varphi) e^{-iEt/\hbar},$$

their spatial part F is known to obey the reduced equation $\nabla^2 F + k^2 F = 0$, with $k^2 \equiv p^2/\hbar^2$ and $p^2 = 2mE$ (quantity $p \equiv |\mathbf{p}|$ being the particle momentum, and therefore $k \equiv |\mathbf{k}|$ the total wavenumber). Such a reduced equation is nothing but the Helmholtz equation, for which various simple localized-beam solutions are already known: In particular, the so-called Bessel beams, which have been experimentally produced since long. Actually, let us look —as usual— for factorized solutions (in the simple case of cylindrical symmetry w.r.t. the z -axis), by supposing the constant longitudinal wavenumber $k_z \equiv p_z/\hbar$. [Since the present formalism is used both in quantum mechanics and in electromagnetism, with a difference in the customary nomenclature, for clarity's sake let us here stress that $k \equiv p/\hbar$; $k_\rho \equiv k_\perp \equiv p_\perp/\hbar$; $\omega \equiv E/\hbar$; while $k_z \equiv k_\parallel = p_\parallel/\hbar \equiv p_z/\hbar$ is often represented by the (for us) ambiguous symbol β]. As a consequence, the (transverse) wavefunction obeys a Bessel differential equation, in which it enters the constant transverse wavenumber $k_\rho \equiv p_\rho/\hbar$ with the *condition* $k_\rho^2 = k^2 - k_z^2 \equiv 2mE/\hbar^2 - k_z^2$. To avoid any divergencies, it must be $k_\rho^2 \geq 0$, that is, $k^2 \geq k_z^2$; namely, it must hold [see Fig.1 in Ref.[3]] the constraint

$$E \geq \frac{p_z^2}{2m}.$$

A simple solution is therefore [$p \equiv \hbar k$]:

$$\psi(\rho, z; t) = J_0(\rho p_\rho/\hbar) \exp[i(zp_z - Et)/\hbar] \quad (98)$$

together with the above condition. *Equation (103) can be regarded as a Bessel beam solution to the Schroedinger equation* [the other Bessel functions are not acceptable here, because of their divergence at $\rho = 0$ or for $\rho \rightarrow \infty$], with forward propagation (i.e., positive z direction) for $k_z > 0$. This result is not surprising, since —once we suppose the whole time variation to be expressed by the function $\exp[i\omega t]$ — both the ordinary wave equation and the Schroedinger equation transform into the Helmholtz equation. Actually, the only difference between the Bessel beam solutions to the wave equation

and to the Schroedinger equation consists in the different relationships among frequency, longitudinal, and transverse wavenumber; in other words (with $E \equiv \omega\hbar$):

$$p_\rho^2 = E^2/c^2 - p_z^2 \quad \text{for the wave equation;} \quad (99)$$

$$p_\rho^2 = 2mE - p_z^2 \quad \text{for the Schroedinger equation.} \quad (100)$$

In the case of beams, the experimental production of NDSs to the Schroedinger equation can be *similar* to the one exploited for the NDSs to the wave equations (e.g., in Optics, or Acoustics): Cf., e.g. Figure 1.2 in the first one of Refs.[52], and refs. therein, where the simple case of a source consisting in an array of circular slits, or rings, were considered.[‡] In the Table we refer to a Bessel beam of photons, and a Bessel beam of (e.g.) electrons, respectively. We list therein the relevant quantities having a role, e.g., in Electromagnetism, and the corresponding ones for the Schroedinger equation's spatial part $\hbar^2\nabla^2 F + 2mEF = 0$, with $F = R(\rho) Z(z)$. The second and the fourth lines have been written down for the so-called simple Durnin et al.'s case, when the Bessel beam is produced by an annular slit (illuminated by a plane wave) located at the focus of a lens[45, 46, 47, 48].

WAVE EQUATION	SCHROEDINGER EQUATION
$k = \frac{\omega}{c}$	$p = \sqrt{2mE}$
$k_\rho \simeq \frac{r}{f} k$	$p_\rho \simeq \frac{r}{f} p$
$k_\rho^2 = \frac{\omega^2}{c^2} - k_z^2$	$p_\rho^2 = 2mE - p_z^2$
$k_z^2 = \frac{\omega^2}{c^2} (1 - \frac{r^2}{f^2})$	$p_z^2 = 2mE(1 - \frac{r^2}{f^2})$

In this Table, quantity f is the focal distance of the lens (for instance, an ordinary lens in optics; and a magnetic lens in the case of Schroedinger charged wavepackets), and r is the radius of the considered ring. [In connection with the last line of the Table, let us recall that in the wave equation case the phase-velocity ω/k_z is almost independent of the frequency (at least for limited frequency intervals, like in optics), and one gets a constant group-velocity and an easy way to build up X-shaped waves. By contrast, in the Schroedinger case, the phase-velocity of each (monochromatic) Bessel beam depends on the frequency, and this makes it difficult to generate an ‘‘X-wave’’ (i.e., a wave depending on z and t only via the quantity $z - Vt$) by using simple methods, as Durnin et al.'s, based on Bessel beams superposition. In the case of charged particles, one should compensate such a velocity variation by suitably modifying the focal distance f of the Durnin's lens, e.g. on having recourse to an additional magnetic, or electric, lens.]

Before going on, let us stress that one could easily eliminate the restriction of axial symmetry: In such a case, in fact, solution (103) would become

[‡]For pulses, however, the generation technique must deviate from Optics', since in the Schroedinger equation case the phase velocity of the Bessel beams produced through an annular slit would depend on the energy.

$$\psi(\rho, z, \varphi; t) = J_n(\rho p_\rho/\hbar) e^{izp_z/\hbar} e^{-iEt/\hbar} e^{in\varphi} ,$$

with n an integer. The investigation of not cylindrically-symmetric solutions is interesting especially in the case of localized *pulses*: and we shall deal with them below.

10.2 Exact non-diffracting solutions to the Schroedinger equation

Coming to the problem of finding out “soliton-like” solutions to the *ordinary* Schroedinger equation, let us switch to a more comprehensive formalism. Namely, in cylindrical coordinates and neglecting evanescent waves, a quite general function ψ of ρ, ϕ, z and t , expressed in terms of Fourier and Hankel transformations, can be written as:

$$\Psi(\rho, \phi, z, t) = \sum_{n=-\infty}^{\infty} \left[\int_0^{\infty} dk_\rho \int_{-\infty}^{\infty} dk_z \int_{-\infty}^{\infty} d\omega k_\rho A'_n(k_\rho, k_z, \omega) J_n(k_\rho \rho) e^{ik_z z} e^{-i\omega t} e^{in\phi} \right] . \quad (101)$$

Notice that the last equation is nothing but Eq.(5), by us considered in subsection 1.3 when having in mind a rather general, ideal solution to linear, homogeneous wave equations in free space (still disregarding the evanescent sector). The essential point, for Eq.(101) to represent a (general) solution to the Schroedinger equation, is imposing now that the $A_n(k_z, \omega)$ be given by

$$A'_n(k_\rho, k_z, \omega) = A_n(k_z, \omega) \delta \left[k_\rho^2 - \left(\frac{2m\omega}{\hbar} - k_z^2 \right) \right] . \quad (102)$$

We request moreover that

$$A_n(k_z, \omega) = \sum_{m=-\infty}^{\infty} S_{mn} \delta [\omega - (Vk_z + b'_m)] , \quad (103)$$

with

$$b'_m = \frac{2m\pi V}{\Delta z_0} . \quad (104)$$

The last two equations guarantee that the general solution (101) to Eq.(97) is a NDW, that is, a wave capable of keeping indefinitely its spatial shape while propagating. Let us recall that such a property, when assuming propagation in the z direction, may be mathematically expressed as in Eq.(7) of Subsection 1.3, where Δz_0 is a chosen length, and V is the pulse peak-velocity, with $0 \leq V \leq \infty$. For the moment, the meaning of the spectral parameters k_z, k_ρ, ω appearing above is not important, since they are dumb integration variables.

Notice that in the general solution (101), together with Eqs.(102-104), all Bessel functions $J_n(k_\rho \rho)$, with any n , appear. Just for simplicity, however, we can choose

$$S_{mn} = S'(\omega) \delta_{0n} \delta_{lm} , \quad (105)$$

where the *delta*'s are now Kronecker's symbols, and l is a positive integer; so as to reduce ourselves to the mere case of zeroth-order Bessel functions. Since we are now dealing with quantum mechanics, let us go on to the new notations

$$k \equiv p/\hbar; \quad k_\rho \equiv p_\rho/\hbar; \quad k_z \equiv p_z/\hbar; \quad \omega \equiv E/\hbar$$

and put $b_l' = 2l\pi V/\Delta z_0 \equiv b/\hbar$.

Since the present formalism is used both in quantum mechanics and in electromagnetism, with a difference in the customary nomenclature, for clarity's sake let us repeat once more that $k \equiv p/\hbar$; $k_\rho \equiv k_\perp \equiv p_\rho/\hbar$; $\omega \equiv E/\hbar$; while $k_z \equiv k_\parallel = p_\parallel/\hbar \equiv p_z/\hbar$.

We can now integrate Eq.(101) in k_ρ and in k_z , obtaining non-diffracting solutions to the Schrodinger equation as the following superpositions (integrations over the frequency, or the energy) of Bessel-beam solutions [with $b \geq 0$]:

$$\Psi(\rho, z, \zeta) = e^{\frac{-ib}{\hbar V}z} \int_{E_-}^{E_+} dE J_0(\rho p_\rho/\hbar) S(E) e^{i\frac{E}{\hbar V}\zeta} , \quad (106)$$

where it is still

$$\zeta \equiv z - Vt , \quad (107)$$

while

$$p_\rho = \frac{1}{V} \sqrt{-E^2 + (2mV^2 + 2b)E - b^2} \quad (108)$$

and

$$E_\pm = mV^2 \left(1 \pm \sqrt{1 + \frac{2b}{mV^2}} \right) + b . \quad (109)$$

Notice that the in Eq.(106) [as well as in equations below like (111)], the solution Ψ depends on z , besides via ζ , only via a phase factor; the modulus $|\Psi|$ of Ψ goes on depending on z (and on t) only through the variable $\zeta \equiv z - Vt$. This means, as we already know, that the magnitude of each solution does not change during propagation: that is, the solutions are NDWs and keep their shape while traveling.

The simple integral solution (106), which yields non-diffracting solutions with azimuthal symmetry, admits of a simple physical interpretation: It implies integrating the Bessel beams $J_0(\rho p_\rho/\hbar) \exp[i\frac{p_z}{\hbar}\zeta] \exp[i\frac{E}{\hbar}t]$, with $p_\rho = \sqrt{2mE - p_z^2}$, in the interval $E_- \leq E \leq E_+$, along the *straight line* $E = Vp_z + b$: This is known to eliminate evanescent waves.

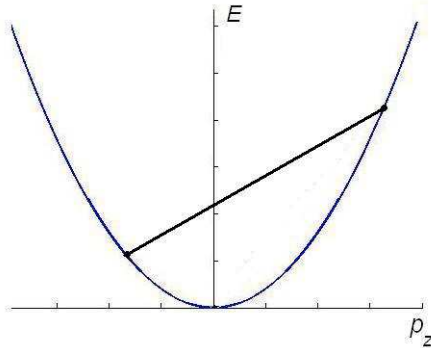


Figure 20: The allowed region is the one internal to the parabola, since (to avoid divergencies) it must be $E \geq p_z^2/(2m)$. In this case, the parabola and the chosen straight-line have equations $E = p_z^2/(2m)$ and $E = Vp_z + b$, respectively. The two values of the intersections of this straight-line with the parabola are given in Eq.(109). Inside the parabola $p_\rho^2 \geq 0$.

Examples — An interesting solution to Eq.(106) is for instance obtained when assuming the *real* exponential spectrum

$$S(E) = s_0 \exp[a(E - E_+)] , \quad (110)$$

a and of E_+ . On integrating[3], we get [\mathcal{N} being a constant]:

$$\Psi(\rho, \eta, \zeta) = \mathcal{N} s_0 2V \sqrt{P} \exp[i \frac{mV}{\hbar} \eta] \exp[-aV \sqrt{P}] \frac{\sin Y}{Y} , \quad (111)$$

where

$$Y \equiv \frac{\sqrt{P}}{\hbar} \sqrt{\rho^2 - (\hbar a V + i\zeta)^2} , \quad (112)$$

and $P \equiv m^2 V^2 + 2mb$, while $\eta \equiv z - vt$ is a function of b . Notice that for $a = 0$, one ends up with a solution similar to Mackinnon's[31]. Equations (111,112) are the simplest closed-form nondiffracting solution to the Schroedinger equation: In Figs.3 of Ref.[3] we have depicted his square magnitude, when choosing for simplicity $b = 0$ [namely, Fig.3a therein corresponds to $a = E_+/5$, while Fig.3b therein corresponds to $a = 5E_+$].

Some physical (interesting) comments on such results will appear elsewhere. Here, let us only add a few brief comments, illustrated by some more Figures. Let us first recall that the Non-diffracting Solutions to the ordinary wave equations resulted to be roughly *ball-like* when their peak-velocity is subluminal[19, 92], and *X-shaped*[9, 14, 92] when superluminal. Now, let us see what happens in the different case of the Schroedinger equation. Normalizing ρ and ζ , we can write Eq.(112) as

$$Y = \sqrt{\rho'^2 - (\bar{A} + i\zeta')^2}$$

with $\rho' \equiv \sqrt{P}\rho/\hbar$ and $\zeta' \equiv \sqrt{P}\zeta/\hbar$, while $\bar{A} \equiv aA = \sqrt{P}aV$. For simplicity, let us stick to the case $b = 0$; therefore, the simple relation will hold: $\bar{A} = maV^2$. For the Schroedinger equation, we can observe that:

(i) If we choose $\bar{A} = 0$, which can be associated with $V = 0$, we get the solutions in Fig.21b: that is, a mainly ball-like structure (even if, differently from the ordinary wave equation cases, an X-shaped structure does timidly start to appear).

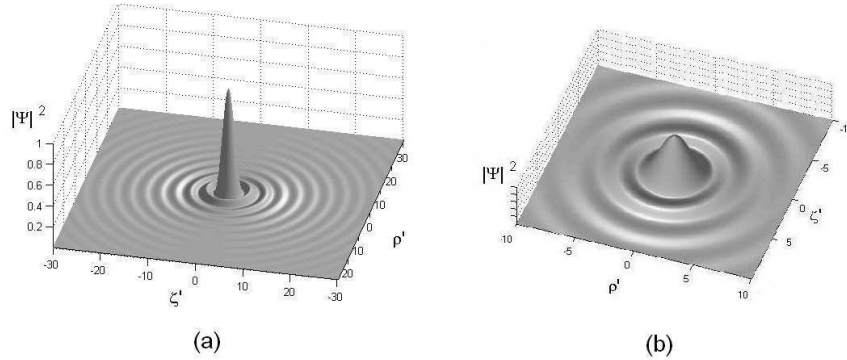


Figure 21: In these, and the following Figure, we depict the square magnitude of elementary solutions of the type (111), corresponding to the *real* spectrum $S(u) = s_0 \exp[(E - E_+)a]$, as a function of $\rho' \equiv \rho\sqrt{P}/\hbar$ and of $\zeta' \equiv \zeta\sqrt{P}/\hbar$. Quantity a is a positive number (when $a = 0$ one ends up with a solutions similar to Mackinnon's[31], while b for simplicity has been chosen equal to zero. Figure (a) corresponds to $a = E_+/5$. For figure (b), normalized with respect to ρ and ζ , we have still assumed for simplicity $b = 0$, so that $\bar{A} = maV^2$: More precisely, it refers to $\bar{A} = 0$ and does clearly show the “ball-like” structure one expects in such a case. It should be however noted that, for the Schroedinger equation, also an X-shaped structure is always appearing —more evident here in figure (a),— even in the most ball-like solutions.

(ii) If we increase by contrast the value of \bar{A} , by choosing e.g. $\bar{A} = 20$ (which can be associated with larger speeds), one notices that now also the X-shaped structure does evidently contribute: See, e.g., Fig.22.

(iii) To have a preliminary idea of the “internal structure” of our soliton-like solutions to the (ordinary) Schroedinger equation, we have to plot, instead of the square magnitude of Ψ , its real or imaginary part: In Figs.6 of Ref.[3] we chose the square of its real part. Then, even in the $\bar{A} = 0$ case, one can start to see in those figures the appearance of the X shape, which becomes more and more evident as the value of \bar{A} increases. We confine ourselves here to stress that the (square of the) real part of Ψ does show, in 3D, also some

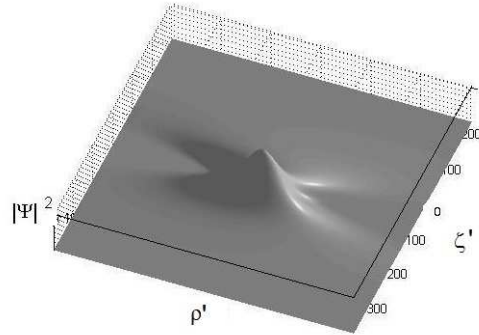


Figure 22: The solution, under all the previous conditions, with an increased value of \bar{A} , namely with $\bar{A} = 20$. An X-shaped structure more evidently appears, contributing in a more clear way to the general form of the solution (see the text).

“internal oscillations”: see, e.g., Fig.23 corresponding to the value $\bar{A} = 5$. We shall face elsewhere topics like their possible connections with the de Broglie picture of quantum particles.

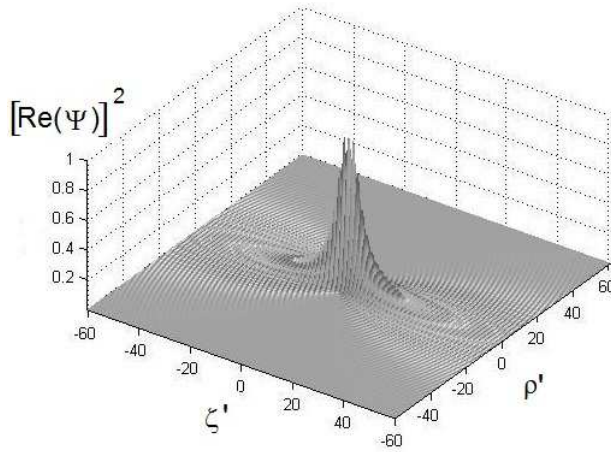


Figure 23: The (square of the) real part of Ψ shows, in 3D, also some “internal oscillations”: this Figure corresponds, e.g., to the value $\bar{A} = 5$.

10.3 A general exact Localized Solution

Let us go back to the choice of spectrum $S(E)$. Since in our equation (106) the integration interval is limited $[E_- < E < E_+]$, in such an interval *any* spectral function $S(E)$ can be

expanded into the Fourier series

$$S(E) = \sum_{n=-\infty}^{\infty} a_n e^{i\frac{2\pi}{D}nE}, \quad (113)$$

with

$$a_n = \frac{1}{D} \int_{E_-}^{E_+} dE S(E) e^{-i\frac{2\pi}{D}nE}, \quad (114)$$

quantity $S(E)$ being an *arbitrary* function, and D being still defined as $D \equiv E_+ - E_-$. Inserting Eq.(113) into Eq.(114), and following[3] the same procedure exploited in the previous Subsection, we get the *general exact non-diffracting solution* to the Schroedinger equation in the form

$$\Psi(\rho, \eta, \zeta) = \mathcal{N} 2A e^{i\frac{mV}{\hbar}\eta} \sum_{n=-\infty}^{\infty} a_n \exp\left[i\frac{2\pi}{D}nB\right] \frac{\sin Z}{Z}, \quad (115)$$

where

$$Z \equiv \sqrt{\left(\frac{A}{\hbar V}\zeta + n\pi\right)^2 + \frac{P}{\hbar^2}\rho^2}. \quad (116)$$

and $A = V\sqrt{P}$; $B = mV^2 + b$, and \mathcal{N} is a suitable normalization constant. Notice that solution (115) yields non-diffracting solutions with azimuthal symmetry for whatever spectrum $S(E)$ in Eq.(106). It is moreover worthwhile to note that, even when truncating the series in Eq.(20) at a certain value $n = N$, the solutions obtained is *still* an exact non-diffracting solution to the Schroedinger equation.

We already mentioned the problem of producing Bessel beams of electrons, instead of optical Bessel beams. As to the possible generating set-ups, an interesting problem from the experimental point of view is that in Optics one starts usually from a laser source; in the case of quantum mechanics, one might have recourse to “laser beams of particles”, as the ones under investigation since more than a decade.

11 A brief mention of further topics

11.1 Airy and Airy-types waves

Many non-diffracting (especially X-shaped) solutions have been constructed for the linear[43] or nonlinear[44] equations that in Optics bear the name of “*Schroedinger equation*”, even if they are mathematically very different from the ordinary Schroedinger’s.

Moreover, a special kind of non-diffracting packet solutions, in terms of Airy functions, were found in the seventies for the case of the actual 1D Schroedinger equation, and extended later on to the 3D case. All that has been recently applied to the case of Optics, originating the discovery of Airy-type waves, now well-known for their remarkable properties[147, 148, 149, 150, 151]: Such Airy waves being solutions, once more, to the so-called (linear) “Schroedinger equation” of Optics.

We wish to repeat here this information, for its intrinsic interest and its relevance, and for the fact that one —or rather two— of the following Chapters of this Book will be mainly devoted to the Airy waves.

The results presented above, in Sect.10 of this Chapter, are rather different, however, from the ones found in Optics, both for the mentioned fact that the optical Schroedinger equation is mathematically different from the ordinary Schroedinger equation, and for the fact that our approach and methods are quite different from the ones adopted in Optics.

11.2 “Soliton-like” solutions to the Einstein equations of General Relativity, and Gravitational waves

Some interesting progress has been performed by one of us [MZR] even in the sector of the Einstein (non-linearized) equations of General Relativity, finding out therefore new possible solutions for gravitational waves. But there is no room here for presenting details.

11.3 Super-resolution

Strong super-resolution effects can be attained by suitable superpositions of evanescent Bessel beams. But this topic too will be reviewed elsewhere, for the tyranny of space.

Acknowledgements

For useful discussions the authors are grateful, among the others, to M.Assis, R.G.Avendaño, M.Balma, I.A.Besieris, R.Bonifacio, D.Campbell, R.Chiao, C.Conti, A.Friberg, D.Faccio, F.Fontana, P.Hawkes, R.Grunwald, G.Kurizki, M.Mattiuzzi, P.Milonni, J.L.Prego-Borges, P.Saari, A.Shaarawi, M.Tygel, A.Utkin and R.Ziolkowski. *Due to reasons of space, many important references had to be skipped in this introductory Chapter: We apologize with the relevant Authors.* This paper has been written as the introductory chapter (Chap.1) of a book on Non-Diffracting Waves published (2014) by J.Wiley-VCH, Berlin; and will constitute a part of a much longer Review (in preparation).

References

- [1] *Localized Waves*, ed. by H.E.Hernández-Figueroa, M.Zamboni-Rached, and E.Recami (J.Wiley; New York, 2008), book of 386 pages.
- [2] E.Recami and M.Zamboni-Rached: “Non-diffracting waves, and ‘Frozen Waves: An Introduction, 121 pages online in *Geophysical Imaging with Localized Waves*, Sanya, China, 2011 [UCSC, S.Cruz, Cal.], and refs. therein; available at <http://es.ucsc.edu/~acti/sanya/SanyaRecamiTalk.pdf>
- [3] M.Zamboni-Rached and E.Recami: “Soliton-like solutions to the ordinary Schroedinger Equation within standard QM”, *J. Mathem. Physics* 53 (2012) 052102 [9 pages], DOI 10.1063/1.4705693: cover article.
- [4] M.Zamboni-Rached, E.Recami and H.E.Hernández-Figueroa: “Theory of ‘Frozen Waves’” [e-print physics/0502105], *Journal of the Optical Society of America A*11 (2005) 2465-2475.
- [5] M.Zamboni-Rached, “Diffraction-attenuation resistant beams in absorbing media”, *Opt. Express* 14 (2006) 1804-1809 [paper chosen for mention also in the *Virtual Journal for Biomedical Optics*, and in *Laser Focus World*, Section “new bracks”].
- [6] M.Zamboni-Rached: “Stationary optical wave fields with arbitrary longitudinal shape by superposing equal frequency Bessel beams: Frozen Waves”, *Optics Express* 12 (2004) 4001-4006.
- [7] L.J.Prego, M.Zamboni-Rached, H.E.Hernández-Figueroa and E.Recami: “Producing Acoustic Frozen Waves: Simulated Experiments”, submitted to *IEEE Trans. Ultrason. Ferroel. Freq. Control* (2012).
- [8] E.Recami, M.Zamboni-Rached, H.E.Hernández-Figueroa et al.: “Method and Apparatus for Producing Stationary (Intense) Wavefields of arbitrary shape”, **Patent**, application no. US-2011/0100880-A1, publication date 05/05/11; the sponsor being “Bracco Imaging, Spa”.
- [9] J.-y. Lu and J.F.Greenleaf: “Nondiffracting X-waves: Exact solutions to free-space scalar wave equation and their finite aperture realizations”, *IEEE Transactions in Ultrasonics Ferroelectricity and Frequency Control* 39 (1992) 19-31; and refs. therein.
- [10] J.-y. Lu and J.F.Greenleaf: “Experimental verification of non-diffracting X-waves”, *IEEE Transactions in Ultrasonics Ferroelectricity and Frequency Control* 39 (1992) 441-446.
- [11] E.Recami and M.Zamboni-Rached: “Localized Waves: A Review”, *Advances in Imaging & Electron Physics (AIEP)* 156 (2009) 235-355 [121 printed pages).

- [12] M.Zamboni-Rached, E.Recami and H.E.Hernández-Figueroa: “New localized Superluminal solutions to the wave equations with finite total energies and arbitrary frequencies,” *European Physical Journal D21* (2002) 217-228.
- [13] E.Recami, M.Zamboni-Rached, K.Z.Nobrega, C.A.Dartora and H.E.Hernández-Figueroa: “On the Localized Superluminal Solutions to the Maxwell Equations”, *IEEE Journal of Selected Topics in Quantum Electronics* 9 (2003) 59-73.
- [14] E.Recami: “On localized X-shaped Superluminal solutions to Maxwell equations,” *Physica A* 252 (1998) 586-610; and refs. therein.
- [15] See also J.-y.Lu, J.F.Greenleaf and E.Recami, “Limited diffraction solutions to Maxwell (and Schroedinger) equations” [Lanl Archives e-print physics/9610012], Report INFN/FM-96/01 (I.N.F.N.; Frascati, 1996).
- [16] See also R.W.Ziolkowski, I.M.Besieris and A.M.Shaarawi, *J. Phys. A: Math.Gen.* **33** (2000) 7227-7254.
- [17] H.Bateman: *Electrical and Optical Wave Motion* (Cambridge Univ.Press; Cambridge, 1915).
- [18] R.Courant and D.Hilbert: *Methods of Mathematical Physics*, vol.2, p.761 (J.Wiley; New York, 1966).
- [19] M.Zamboni-Rached and E.Recami: “Sub-luminal Wave Bullets: Exact Localized subluminal Solutions to the Wave Equations” [e-print arXiv:0709.2372], *Physical Review A* 77 (2008) 033824.
- [20] H.Sõnajalg and P.Saari, “Suppression of temporal spread of ultrashort pulses in dispersive media by Bessel beam generators”, *Optics Letters* 21 (1996) 1162-1164.
- [21] H.Sõnajalg, M.Ratsep and P.Saari, “Demonstration of Bessel-X pulse propagating with strong lateral and longitudinal localization in a dispersive medium”, *Optics Letters* 22 (1997) 310-312.
- [22] M.Zamboni-Rached, K.Z.Nóbrega, H.E.Hernández-Figueroa and E. Recami, ”Localized Superluminal solutions to the wave equation in (vacuum or) dispersive media, for arbitrary frequencies and with adjustable bandwidth”, *Optics Communications* 226 (2003) 15-23.
- [23] C.Conti, S.Trillo, G.Valiulis, A.Piskarkas, O. van Jedrkiewicz, J.Trull and P.Di Trapani, “Non-linear electromagnetic X-waves”, *Phys. Rev. Lett.* 90 (2003) 170406.
- [24] J.Salo, J.Fagerholm, A.T.Friberg and M.M.Salomaa: “Nondiffracting bulk-acoustic X-waves in crystals”, *Phys. Rev. Lett.* 83 (1999) 1171-1174.

- [25] J.Salo and M.M.Saloma: “Nondiffracting waves in anisotropic media”, Phys. Rev. E67 (2003) 056609
- [26] J.Salo and A.T.Friberg: “Propagation-invariant fields: Rotationally periodic and anisotropic nondiffracting waves”, Chap.5 in the book [1].
- [27] C.J.R.Sheppard: “Generalized Bessel pulse beams”, J. Opt. Soc. Am. A19 (2002) 2218-2222.
- [28] S.Longhi: “Localized subluminal envelope pulses in dispersive media”, Opt. Letters 29 (2004) 147-149.
- [29] J.Salo and M.M.Saloma: “Subsonic nondiffracting waves”, Acoustic Res. Lett. Online 2(1) (2001) 31-36;
- [30] J.-y. Lu and J.F.Greenleaf: “Comparison of sidelobes of limited diffraction beams and localized waves”, Acoustical Imaging 21 (1995) 145-152.
- [31] L.Mackinnon: “A nondispersive de Broglie wave packet”, Found. Phys. 8 (1978) 157.
- [32] W.A.Rodrigues, J.Vaz and E.Recami: “Free Maxwell equations, Dirac equation, and non-dispersive de Broglie wave packets”, in *Courants, Amers, Écueils en Microphysique*, ed. by G. & P.Loachak (Paris, 1994), pp.379-392.
- [33] J.-y. Lu and J.F.Greenleaf: “Comparison of sidelobes of limited diffraction beams and localized waves”, in *Acoustic Imaging*, vol.21, ed. by J.P.Jones (Plenum; New York, 1995), pp.145-152-
- [34] J.Salo and M.M.Saloma: “Subsonic nondiffracting waves”, Acoustics Res. Lett. Online 2(1) (2001) 31-36.
- [35] S.Longhi: “Localized subluminal envelope pulses in dispersive media”, Opt. Lett. 29 (2004) 147-149.
- [36] M.Zamboni-Rached, E.Recami and I.M.Besieris: “Cherenkov radiation vs X-shaped Localized Waves”, *J. Opt. Soc. Am.* A27 (2010) 928-934.
- [37] M.Zamboni-Rached, E.Recami and I.M.Besieris: “Further comments on Cherenkov versus X-waves”, *Journal of the Optical Society of America* A29 (2012) 2536-2541 [1084-7529/12/120001-01].
- [38] A.B.Utkin: “Droplet-shaped waves: causal finite-support analogs of X-shaped waves,” *J. Opt. Soc. Am.* A29 (2012) 457-462.
- [39] Z.Bouchal, J.Wagner and M.Chlup: “Self-reconstruction of a distorted nondiffracting beam”, *Optics Communications* 151 (1998) 207-211.

- [40] R.Grunwald, U.Griebner, U.Neumann and V.Kebbel, “Self-reconstruction of ultrashort-pulse Bessel-like X-waves”, CLEO/QELS Conference (San Francisco; 2004), paper no.CMQ7.
- [41] J.N.Brittingham: “Focus wave modes in homogeneous Maxwell’s equations: transverse electric mode”, J. Appl. Phys. 54 (1983) 1179-1189.
- [42] A.Sezginer: “A general formulation of focus wave modes”, J. Appl. Phys. 57 (1985) 678-683.
- [43] J.H.McLeod: “The Axicon: A new type of optical element”, J. Opt. Soc. Am. 44 (1954) 592-597;
- [44] J.H.McLeod: “Axicons and their use”, J. Opt. Soc. Am. 50 (1960) 166-169;
- [45] C.J.R.Sheppard and T.Wilson: “Gaussian-beam theory of lenses with annular aperture”, IEEE Journal on Microwaves, Optics and Acoustics 2 (1978) 105-112; 163-166.
- [46] C.J.R.Sheppard: “The use of lenses with annular aperture”, Optik 48 (1977) 329-334.
- [47] J.Durnin, J.J.Miceli and J.H.Eberly: “Diffraction-free beams”, Physical Review Letters 58 (1987) 1499-1501.
- [48] J.Durnin: “Exact solutions for nondiffracting beams: I. The scalar theory”, Journal of the Optical Society of America A4 (1987) 651-654.
- [49] M.Zamboni-Rached: “Localized solutions: Structure and Applications”, M.Sc. thesis (Phys. Dept., Campinas State University, 1999).
- [50] M.Zamboni-Rached, “Localized waves in diffractive/dispersive media”, PhD Thesis, Aug.2004, Universidade Estadual de Campinas, DMO/FEEC [download at <http://libdigi.unicamp.br/document/?code=vtls000337794>], and refs. therein.
- [51] C.A.Dartora, M.Zamboni-Rached and E.Recami: “General formulation for the analysis of scalar diffraction-free beams using angular modulation: Mathieu and Bessel beams”, Optics Communications 222 (2003) 75-85.
- [52] E.Recami, M.Zamboni-Rached and H.E.Hernández-Figueroa: “Localized waves: A historical and scientific introduction”, introductory Chapter of the book in Ref.[1].
- [53] M.Zamboni-Rached, E.Recami and H.E.Hernández-Figueroa: “Structure of the nondiffracting waves, and some interesting applications”, a Chapter of the book in Ref.[1].

- [54] I.M.Besieris, M.Abdel-Rahman, A.Shaarawi and A.Chatzipetros: “Two fundamental representations of localized pulse solutions of the scalar wave equation”, *Progress in Electromagnetic Research (PIER)* 19 (1998) 1-48.
- [55] R.W.Ziolkowski: “Localized transmission of electromagnetic energy”, *Physical Review A* 39 (1989) 2005-2033.
- [56] I.M.Besieris, A.M.Shaarawi and R.W.Ziolkowski: “A bi-directional traveling plane wave representation of exact solutions of the scalar wave equation”, *J. Math. Phys.* 30 (1989) 1254-1269.
- [57] R.W.Ziolkowski: “Localized wave physics and engineering”, *Physical Review A* 44 (1991) 3960-3984.
- [58] R.Donnely and R.W.Ziolkowski, “Designing localized waves”, *Proc. R. Soc. Lond. A* 440 (1993) 541-565.
- [59] R.W.Ziolkowski, I.M.Besieris and A.M.Shaarawi, “Aperture realizations of exact solutions to homogeneous wave-equations”, *J. Opt. Soc. Am. A* 10 (1993) 75-87.
- [60] S.Esposito: “Classical solutions of Maxwell’s equations with group-velocity different from c , and the photon tunneling effect”, *Phys. Lett. A* 225 (1997) 203-209.
- [61] A.T.Friberg, J.Fagerholm and M.M.Salomaa: “Space-frequency analysis of non-diffracting pulses”, *Optics Communications* 136 (1997) 207-212.
- [62] A.M.Shaarawi and I.M.Besieris: “On the Superluminal propagation of X-shaped localized waves”, *J. Phys. A* 33 (2000) 7227-7254.
- [63] E.Recami: “Superluminal motions? A bird’s-eye view of the experimental status-of-the-art”, *Found. Phys.* 31 (2001) 1119-1135.
- [64] I.Besieris and A.Shaarawi, “Three classes of Courant-Hilbert’s progressing solutions to the scalar wave equation”, *J. Electr. Waves Appl.* 16(8) (2002) 1047-1060.
- [65] M.Zamboni-Rached: “Unidirectional decomposition method for obtaining exact localized wave solutions totally free of backward components”, *Physical Review A* 79 (2009) 013816.
- [66] V.V.Borisov and A.P.Kiselev: “A new class of relatively undistorted progressing waves”, *Appl. Mathem. Lett.* 13 (2000) 83-86.
- [67] A.P.Kiselev and M.V.Perel: “Highly localized solutions of the wave equation”, *J. Math. Phys.* 41 (2000) 1934-1955.

- [68] M.Zamboni-Rached, K.Z.Nobrega, E.Recami and H.E.Hernández-Figueroa: “Superluminal X-shaped beams propagating without distortion along a coaxial guide”, *Physical Review E* 66 (2002) no.036620 [10 pages]; and refs. therein.
- [69] M.Zamboni-Rached, E.Recami and F.Fontana: “Localized Superluminal solutions to Maxwell equations propagating along a normal-sized waveguide”, *Physical Review E* 64 (2001) no.066603 [6 pages].
- [70] M.Zamboni-Rached, F.Fontana and E.Recami: “Superluminal localized solutions to Maxwell equations propagating along a waveguide: The finite-energy case”, *Phys. Rev. E* 67 (2003) no.036620 [7 pages].
- [71] M.Zamboni-Rached, A.Shaarawi and E.Recami: “Focused X-Shaped Pulses”, *Journal of the Optical Society of America A* 21 (2004) 1564-1574.
- [72] A.M.Shaarawi, I.M.Besieris and T.M.Said, “Temporal focusing by use of composite X-waves”, *J. Opt. Soc. Am. A* 20 (2003) 1658-1665.
- [73] M. Zamboni-Rached, H. E. Hernández-Figueroa and E.Recami: “Chirped optical X-shaped pulses in material media”, *J. Opt. Soc. Am. A* 21 (2004) 2455-2463.
- [74] H.Sõnajalg, P.Saari, “Suppression of temporal spread of ultrashort pulses in dispersive media by Bessel beam generators”, *Opt. Letters* 21 (1996) 1162-1164. Cf. also H.Sõnajalg, M.Rätsep and P.Saari: *Opt. Lett.* 22 (1997) 310.
- [75] M.A.Porras, G.Valiulis and P.Di Trapani: “Unified description of Bessel X waves with cone dispersion and tilted pulses”, *Phys. Rev. E* 68 (2003) 016613.
- [76] S.Longhi: “Spatial-temporal Gauss-Laguerre waves in dispersive media”, *Phys. Rev. E* 68 (2003) no.066612 [6 pages].
- [77] M.Zamboni-Rached, E.Recami and M.Balma: “Simple and effective method for the analytic description of important optical beams when truncated by finite apertures”, *Applied Optics* 51 (2012) 3370-3379 [DOI 1559-128X/12/163370-10].
- [78] M. Zamboni-Rached: “Analytical expressions for the longitudinal evolution of non-diffracting pulses truncated by finite apertures,” *J. Opt. Soc. Am. A* 23 (2006) 2166-2176.
- [79] J.-y. Lu, H.-h.Zou and J.F.Greenleaf: “Producing deep depth of field and depth independent resolution in NDE with limited diffraction beams”, *Ultrasonic Imaging* 15 (1993) 134-149.
- [80] M.Zamboni-Rached, E.Recami and M.Balma: “Proposal of apertures for generating non-diffracting beams of microwaves, arXiv:1108.2027 [physics], Aug. 2011.

- [81] M.Zamboni-Rached, E.Recami and M.Balma: “Analytical descriptions of optical beams truncated by finite apertures”, in *Progress in Electromagnetics Research Symposium (PIERS) Proceedings*, Moscow, Russia, Aug. 2012; pp.464-468 [ISSN 1559-9450].
- [82] P.Saari and K.Reivelt: “Evidence of X-shaped propagation-invariant localized light waves”, *Physical Review Letters* 79 (1997) 4135-4138.
- [83] D.Mugnai, A.Ranfagni, and R.Ruggeri: “Observation of Superluminal behaviors in wave propagation”, *Physical Review Letters* 84 (2000) 4830-4833.
- [84] Cf. also H.Valtna, K.Reivelt and P.Saari: “Methods for generating wideband localized waves of superluminal group-velocity”, *Opt. Comm.* 278 (2007) 1-7.
- [85] P.Bowlan, H.Valtna-Luckner, M.Löhmus, P.Piksarv, P.Saari and R.Trebino: “Measuring the spatiotemporal field of ultrashort Bessel X pulses”, *Opt. Lett.* 34 (2009) 2276-2278.
- [86] J.-y. Lu, H.-H.Zou and J.F.Greenleaf: “Biomedical ultrasound beam forming”, *Ultrasound in Medicine and Biology*, vol.20, pp.403-428 (1994).
- [87] J.-y. Lu, H.-h.Zou and J.F.Greenleaf: “Producing deep depth of field and depth independent resolution in NDE with limited diffraction beams”, *Ultrasonic Imaging*, vol.15, pp.134-149, 1993.
- [88] J.E.Curtis, B.A.Koss and D.G.Grier: “Dynamic holographic optical tweezers”, *Optics Communications* 207 (2002) 169-175.
- [89] L.A.Ambrosio and H.E.Hernández-Figueroa: “Gradient forces on double-negative particles in optical tweezers using Bessel beams in the ray optics regime”, *Opt. Express* 18 (2010) 24287-24292.
- [90] M.Zamboni-Rached, L.A.Ambrosio and H.E.Hernández-Figueroa, “Diffraction-attenuation resistant beams: their higher-order versions and finite-aperture generation”, *Appl. Opt.* 49 (2011) 5861-5869.
- [91] *Ettore Majorana - Notes on Theoretical Physics*, edited by S.Esposito, E.Majorana jr., A. van der Merwe and E.Recami (Kluwer; Dordrecht and N.Y., 2003), 512 pages.
- [92] A.O.Barut, G.D.Maccarrone and E.Recami: “On the Shape of Tachyons”, *Nuovo Cimento A*, vol.71, pp.509-533 (1982), and refs. therein.
- [93] J.A.Stratton: *Electromagnetic Theory*, page 356 (McGraw-Hill; New York, 1941).
- [94] E.Recami, M.Zamboni-Rached and C.A.Dartora: “The X-shaped, localized field generated by a Superluminal electric charge” [e-print physics/0210047], *Physical Review E* 69 (2004) 027602.

- [95] P.Hillion: “Arrow Wave modes”, *J. Opt. A: Pure Appl. Opt.* 3 (2001)311-316.
- [96] A.C.Newell and J.V.Molone: *Nonlinear Optics* (Addison & Wesley; Redwood City, CA, 1992).
- [97] J.Durnin, J.J.Miceli and J.H.Eberly: “Comparison of Bessel and Gaussian beams”, *Optics Letters*, vol.13, pp.79-80 (1988).
- [98] P.L.Overfelt and C.S.Kenney: “Comparison of the propagation characteristics of Bessel, Bessel-Gauss, and gaussian beams diffracted by a circular aperture”, *Journal of the Optical Society of America A*, vol.8, pp.732-745 (1991).
- [99] R.Folman and E.Recami: “On the phenomenology of tachyon radiation”, *Found. Phys. Letters* 8 (1995) 127-134.
- [100] I.Besieris and A.Shaarawi, “Paraxial localized waves in free space”, *Opt. Express* 12 (2004) 3848-3864.
- [101] M.A.Porras, S.Trillo, C.Conti and P.Di Trapani: “Paraxial envelope X waves”, *Opt. Lett.* 28 (2003) 1090-1092.
- [102] I.S.GradshTEyn and I.M.Ryzhik: *Integrals, Series and Products*, 5th edition (Ac.Press; New York, 1965).
- [103] J.W.Goodman: *Introduction to Fourier Optics*, 2nd edition (McGraw-Hill; New York, 1996).
- [104] F.Gori and G.Guattari: “Bessel-Gauss beams”, *Optics Communications* 64 (1987) 491-495.
- [105] J.Salo and M.M.Salomaa: “Subsonic nondiffracting waves”, *Acoustics Res. Lett. Online* 2(1) (2001) 31-36.
- [106] M.Zamboni-Rached and H.E.Hernández-Figueroa: “A rigorous analysis of Localized Wave propagation in optical fibers”, *Opt. Comm.* 191 (2000) 49-54.
- [107] C.A Dartora, K.Z.Nóbrega, A.Dartora, G.A.Viana and H.T.S.Filho: “A general theory for the frozen waves and their realizations through finite apertures”, *Opt. Commun.* 265 (2006) 481; “Study of Frozen Waves’ theory through continuous superpositions of Bessel beams”, *Optics and Laser Tech.* 39 (2007) 1370.
- [108] M.Zamboni-Rached and H.E.Hernández-Figueroa: “A rigorous analysis of Localized Wave propagation in optical fibers”, *Opt. Comm.* 191 (2000) 49-54.
- [109] T.A.Vieira, M.R.R.Gesualdi, and M.Rached: “Frozen waves: Experimental generation”, *Opt. Lett.* 37, 2034-2036 (2012).

- [110] E.Recami: “Classical Tachyons and Possible Applications”, *Rivista Nuovo Cim.* 9(6) (1986) 1-178, issue no.6; and refs. therein.
- [111] E.Recami and W.A.Rodrigues: “A Model Theory for Tachyons in Two Dimensions”, in *Gravitational Radiation and Relativity* (vol.3 of the Proceedings of the Sir Arthur Eddington Centenary Symposium), ed. by J.Weber and T.M.Karade (World Scientific; Singapore, 1985), pp.151-203.
- [112] See, e.g., E.Recami (editor): *Tachyons, Monopoles, and Related Topics* (North-Holland; Amsterdam; 1978), pp.X + 285.
- [113] E.Recami and R.Mignani: “Magnetic Monopoles and Tachyons in Special Relativity”, *Physics Letters B*62 (1976) 41-43.
- [114] E.Recami and R.Mignani: *Rivista Nuovo Cim.* 4 (1974) 209-290; E398.
- [115] R.Mignani and E.Recami: “Generalized Lorentz Transformations and Superluminal Objects in Four Dimensions”, *Nuovo Cimento A*14 (1973) 169-189; A16, 206.
- [116] P.Saari and K.Reivelt: “Generation and classification of localized waves by Lorentz transformations in Fourier space”, *Phys. Rev.* E69 (2004) 036612; and refs. therein.
- [117] J.Arlt, V.Garcés-Chavez, W.Sibbett and K.Dholakia: “Optical micromanipulation using a Bessel light beam”, *Optics Communications* 197 (2001) 239-245.
- [118] R.M.Herman and T.A.Wiggins: “Production and uses of diffractionless beams”, *Journal of the Optical Society of America A*8 (1991) 932-942.
- [119] V.Garcés-Chavez, D.McGloin, H.Melville, W.Sibbett and K.Dholakia: “Simultaneous micromanipulation in multiple planes using a self-reconstructing light beam”, *Nature* 419 (2002) 145-147.
- [120] V.Garcs-Chvez, D.Roskey, M.D.Summers, H.Melville, D.McGloin, E.M.Wright and K.Dholakia: “Optical levitation in a Bessel light beam”, *Appl. Phys. Lett.* 85 (2004) 4001-4003.
- [121] G.Milne, K.Dholakia, D.McGloin, K.Volke-Sepulveda and P. Zemnek: “Transverse particle dynamics in a Bessel beam”, *Opt. Express* 15 (2007) 13972-13987.
- [122] K.C.Neuman, and S.M.Block: “Optical trapping”, *Rev. Sci. Instrum.* 75 (2004) 2787-2809.
- [123] A.Ashkin: “Forces of a single-beam gradient laser trap on a dielectric sphere in the ray optics regime”, *Biophys. J.* 61 (1992) 569-582.

- [124] K.Volke-Sepulveda, S.Chávez-Cerda, V.Garcés-Chávez, and K.Dholakia: “Three-dimensional optical forces and transfer of orbital angular momentum from multi-ringed light beams to spherical particles”, J. Opt. Soc. Am. B21 (2004) 1749.
- [125] V.Garcés-Chávez, K.Volte-Sepulveda, S.Chávez-Cerda, W.Sibbett, and K.Dholakia: “Transfer of orbital angular momentum to an optically trapped low-index particle”, Phys. Rev. A66 (2002) 063402.
- [126] A.N.Rubinov, A.A.Afanas’ev, I.E.Ermolaev, Y.A.Kurochkin and S.Y.Mikhnevich: “Localization of spherical particles under the action of gradient forces in the field of a zero-order Bessel beam. Rayleigh-Gans approximation”, J. Appl. Spectrosc. 70 (2003) 565-572.
- [127] G.Gouesbet and G.Grhan: “Sur la gnralisation de la thorie de Lorenz-Mie”, J. Opt. (Paris) 13 (1982) 97-103.
- [128] B.Maheu, G.Gouesbet, and G.Grhan: “A concise presentation of the generalized Lorenz-Mie theory for arbitrary incident profile”, J. Opt. (Paris) 19 (1988) 59-67.
- [129] J.A.Lock and G.Gouesbet: “Generalized Lorenz-Mie theory and applications”, J. Quant. Spectrosc. Radiat. Transf. 110 (2009) 800-807.
- [130] G.Gouesbet: “Generalized Lorenz-Mie theories, the third decade: A perspective”, J. Quant. Spectrosc. Radiat. Transf. 110 (2009) 1223-1238.
- [131] G.Gouesbet, and G.Grhan: *Generalized Lorenz-Mie theories*, Springer-Verlag, 2010.
- [132] G.Gouesbet, G.Grhan and B.Maheu: “Expressions to compute the coefficients g_n^m in the generalized Lorenz-Mie theory using finite series”, J. Opt. (Paris) 19 (1988) 35-48.
- [133] G.Gouesbet, G.Grhan and B.Maheu: “On the generalized Lorenz-Mie theory: first attempt to design a localized approximation to the computation of the coefficients g_n^m ,” J. Opt. (Paris) 20 (1989) 31-43.
- [134] G.Gouesbet, G.Grhan and B.Maheu: “Localized interpretation to compute all the coefficients g_n^m in the generalized Lorenz-Mie theory”, J. Opt. Soc. Am. A7 (1990) 998-1007.
- [135] G.Gouesbet, and J.A.Lock: “Rigorous justification of the localized approximation to the beam-shape coefficients in generalized Lorenz-Mie theory. I. On-axis beams”, J. Opt. Soc. Am. A11 (1994) 2503-2515.
- [136] G.Gouesbet and J.A.Lock: “Rigorous justification of the localized approximation to the beam-shape coefficients in generalized Lorenz-Mie theory. II. Off-axis beams”, J. Opt. Soc. Am. A11 (1994) 2516-2525.

- [137] L.A.Ambrosio and H.E.Hernández-Figueroa: “Integral localized approximation description of ordinary Bessel beams and application to optical trapping forces”, *Biomed. Opt. Express* 2 (2011) 1893-1906.
- [138] K.F.Ren, G.Gouesbet and G.Grhan: “Integral localized approximation in generalized Lorenz-Mie theory”, *Appl. Optics* 37 (1998) 4218-4225.
- [139] L.A.Ambrosio and H.E.Hernández-Figueroa: “Radiation pressure cross section and optical forces over negative refractive index spherical particles by ordinary Bessel beams”, *Appl. Opt.* 50 (2011) 4489-4498.
- [140] R.Li, K.F.Ren, X.Han, Z.Wu, L.Guo and S.Gong: “Analysis of radiation pressure force exerted on a biological cell induced by high-order Bessel beams using Debye series”, *J. Quant. Spectrosc. Radiat. Transf.* (2012), <http://dx.doi.org/10.1016/j.jqsrt.2012.07.030>.
- [141] A.A.R.Neves, A.Fontes, L.A.Padilha, E.Rodriguez, C.H.D.Cruz, L.C.Barbosa and C.L.Cesar: “Exact partial wave expansion of optical beams with respect to an arbitrary origin”, *Opt. Lett.* 31 (2006) 2477-2479.
- [142] A.A.R.Neves, A.Fontes, L.D.Y.Pozzo, A.A.de Thomaz, E.Chillce, E.Rodriguez, L.C.Barbosa and C.L.Cesar: “Electromagnetic forces for an arbitrary optical trapping of a spherical dielectric”, *Opt. Express* 14 (2006) 13101-13106.
- [143] Z.Bouchal and M.Olivk: “Non-diffracting vector Bessel beams”, *J. Modern Opt.* 42 (1995) 1555-1566.
- [144] V.G.Veselago: “The electrodynamics of substances with simultaneously negative values of ϵ and μ ,” *Sov. Phys. Usp.* 10 (1968) 509-514.
- [145] D.R.Smith, W.J.Padilla, D.C.Vier, S.C.Nemat-Nasser and S. Schultz,: “Composite medium with simultaneously negative permeability and permittivity”; *Phys. Rev. Lett.* 84 (2000) 4184-4187.
- [146] R.A.Shelby, D.R.Smith and S.Schultz: “Experimental verification of a negative index of refraction”, *Science* 292 (2001) 77-79.
- [147] G.A.Siviloglu and D.N.Christodoulides: “Accelerating finite energy airy beams”, *Opt. Lett.* 32 (2007) 979-981.
- [148] G.A.Siviloglu, J.Broky, A.Dogariu and D.N.Christodoulides: “Observation of accelerating airy beams”, *Phys. Rev. Lett.* 99 (2007) 213901
- [149] I.M.Besieris and A.M.Shaarawi: “Accelerating Airy wave packets in the presence of quadratic and cubic dispersion”, *Phys. Rev.* E78 (2008) 046605.

- [150] G.A.Siviloglu, J.Broky, A.Dogariu and D.N.Christodoulides: “Ballistic dynamics of airy beams”, *Opt. Lett.* 33 (2008) 207
- [151] A.Lotti, D.Faccio, A.Couairon et al.: “Stationary nonlinear Airy beams”, *Phys. Rev.* A84 (2011) 021807.
- [152] V.S.Olkhovsky and E.Recami: “Recent Developments in the Time Analysis of Tunnelling Processes”, *Physics Reports* 214 (1992) 339-357, and refs. therein.
- [153] V.S.Olkhovsky, E.Recami and J.Jakiel: “Unified time analysis of photon and non-relativistic particle tunneling”, *Physics Reports* 398 (2004) 133-178.
- [154] G.Privitera, E.Recami, G.Salesi and V.S.Olkhovsky: “Tunnelling Times: An Elementary Introduction”, *Rivista Nuovo Cim.* 26 (2003), monographic issue no.4 [54 pages].
- [155] A.P.L.Barbero, H.E.Hernández-Figueroa and E.Recami: “On the propagation speed of evanescent modes”, *Physical Review* E62 (2000) 8628-8635.
- [156] J.-y. Lu and H.Shiping: “Optical X wave communications”, *Optics Communications*, vol.161, pp.187-192 (1999).